sustainability

MDPI

Review

Solar Photovoltaic Power Forecasting: A Review

Kelachukwu J. Iheanetu

Fort Hare Institute of Technology, University of Fort Hare, Alice 5700, South Africa; kiheanetu@ufh.ac.za

Abstract: The recent global warming effect has brought into focus different solutions for combating climate change. The generation of climate-friendly renewable energy alternatives has been vastly improved and commercialized for power generation. As a result of this industrial revolution, solar photovoltaic (PV) systems have drawn much attention as a power generation source for varying applications, including the main utility-grid power supply. There has been tremendous growth in both on- and off-grid solar PV installations in the last few years. This trend is expected to continue over the next few years as government legislation and awareness campaigns increase to encourage a shift toward using renewable energy alternatives. Despite the numerous advantages of solar PV power generation, the highly variable nature of the sun's irradiance in different seasons of various geopolitical areas/regions can significantly affect the expected energy yield. This variation directly impacts the profitability or economic viability of the system, and cannot be neglected. To overcome this challenge, various procedures have been applied to forecast the generated solar PV energy. This study provides a comprehensive and systematic review of recent advances in solar PV power forecasting techniques with a focus on data-driven procedures. It critically analyzes recent studies on solar PV power forecasting to highlight the strengths and weaknesses of the techniques or models implemented. The clarity provided will form a basis for higher accuracy in future models and applications.

Keywords: renewable energy; solar; photovoltaic; forecasting; data-driven; machine learning; modeling

Citation: Iheanetu, K.J. Solar Photovoltaic Power Forecasting: A Review. *Sustainability* **2022**, *14*, 17005. https://doi.org/10.3390/su142417005

Academic Editor: Tamer Khatib

Received: 14 October 2022
Accepted: 14 December 2022
Published: 19 December 2022

1. Introduction

Population growth, modern lifestyle, and advanced technology continue to increase the world's energy demand, particularly electrical energy. Fossil fuel energy sources have been a significant contributor to meeting this energy need, and its by-products lead to global warming. Energy technologies are currently moving toward using renewable energy sources to reduce the impact of global warming. Solar photovoltaic (PV) energy systems are the most favored renewable energy alternatives. Many countries are moving on to the use of solar PV energy generation systems for large-scale electricity generation. This is because it is a clean, renewable energy source with almost zero maintenance costs. It is estimated that solar PV electricity energy generation increased by 23% from 2019 to 2020, to reach a record high of 156 TWh. Solar PV power generation capacity is projected to reach 7000 TWh by 2050 [1]. PV power generation is highly dependent on uncontrolled weather and environmental conditions, such as module temperature, solar irradiance, wind speed, wind pressure and direction, atmospheric temperature, humidity, etc. The output power of a PV system dynamically changes with time due to the variability of the aforementioned environmental factors. Therefore, the accurate forecasting of PV power generation is considerably difficult. The inability to predict PV output power significantly affects its stability, dependability, and scheduling of the power system operation, not to mention the economic benefit [2–4]. Accurately forecasting PV power generation can reduce the effect of PV power uncertainty on the grid, improve system reliability, maintain power quality, and increase the penetration level of PV systems.

Regardless of the numerous advantages of PV power generation systems over other renewable energy sources, there exist several challenges regarding its large-scale integration,

such as changes in solar irradiation, humidity, presence of dust in the air, temperature, and wind speed, which significantly impact the variability of the output power generated by the PV system [5]. Uncertainties in these weather parameters make it challenging to accurately predict the power output expected from solar PV power generation systems [6]. Consequently, it becomes a barrier to efficient electric power utility-grid system planning and pricing.

As more PV power generation systems are integrated into the main energy grid by residential and commercial users, the problem of handling these uncertainties increases. This negatively affects the development and sustainability of solar PV technology as well. Currently, the main solution to the challenges encountered by variable weather conditions has been the use of battery backup systems. The backup system ensures a smooth power supply at the desired level, irrespective of the actual weather condition. However, this becomes an additional system cost, as the battery backup systems are usually expensive. Oftentimes, they are more expensive than the actual solar PV system. In addition, if the weather condition over an extended period is unfavorable, the batteries become discharged, and the systems go offline.

A practical solution to overcome this challenge is efficient forecasting of the PV output power [4,6]. Solar PV power forecasting provides a means by which a reliable estimate of the power from the solar PV plant is obtained after considering the existing weather conditions and system losses. Power plant operators can use the forecasted power for planning, decision-making, and distribution management [7]. Connecting PV power generation systems to the main grid can only be accomplished efficiently, with a forecasted estimate of the yield obtainable during different seasons and times of the day from the solar PV plant. This is the perspective of efficient forecasting, as it enables effective planning and scheduling of the grid-connected power systems. Several attempts have been made to forecast solar PV output power. Several authors and peer-reviewed papers have been published in this regard. Some of the developed techniques have been applied in commercial solar PV design suites and software and are now utilized by utility grid electrical energy planners. Due to the significant amount of work conducted in this aspect, many reviews have been published for ease of appraisal and evaluation of previously applied techniques and procedures [8–12]. In [8], time and spatial forecasting approaches were reviewed, with an emphasis on the short-term time horizon. As stated by the authors, the intended benefit of the work was to assist in short-term energy planning, particularly while still in the project's tender phase. The review in [10] focused on only direct forecasting approaches. It reviewed the techniques applied to the input–output data and pre-processing methods, highlighting the various techniques' strengths and weaknesses. Mellit et al. [11] reviewed the artificial intelligence (AI) techniques applied for solar PV output power forecasting. Their review focused on providing special attention to the AI techniques applied due to the increasing popularity of the methods and the future trends envisaged. The review in [12] briefly highlighted the broad classification of solar PV output power forecasting methods, and further highlighted model selection strategies and indicators.

While some of the above review work focused their review discussions on some event horizon, others focused only on the spatial horizon, and reviewed only some classes of PV output power forecasting. They paid little or no attention to other classes. Thus, there is a need to conduct a comprehensive review of solar PV output power forecasting techniques. Again, there have been recent advances in developing PV forecasting models since the above reviews were published. Thus, this research is focused on providing a more comprehensive and systematic review of recent advances in PV power forecasting, as well as a theoretical foundation for securing the stability of distributed systems. The simulations carried out by electrical power distribution system operators will make advance production of large volumes of (dependable electrical) power possible. This work makes it easy to identify appropriate mitigation measures when designing and building distributed energy systems.

In Section 2 of this work, we present the classification of PV output power forecasting models, and in Section 3, we present the data analytics. Section 4 aims at evaluating the performance of selected forecasting technologies. Section 5 investigates the model optimization procedures, and Section 6 considers the challenges of PV output power forecasting. Finally, conclusions are drawn in Section 7.

2. Classifying PV Output Power Prediction Models Based on the Forecasting Method

Several studies have been conducted in order to develop appropriate forecasting models to accurately predict the power generation of solar PV systems, with minimum complexity and cost. PV output power prediction generally involves three steps. The first is extracting the energy characteristics and analyzing the factors that affect them. The second is choosing the prediction method and optimizing the forecasting model. PV output power forecasting techniques can be broadly classified into three categories—physical, statistical and hybrid—based on the forecasting method used. These broad classifications can be further subdivided based on the actual modeling procedures applied in the literature (Figure 1).

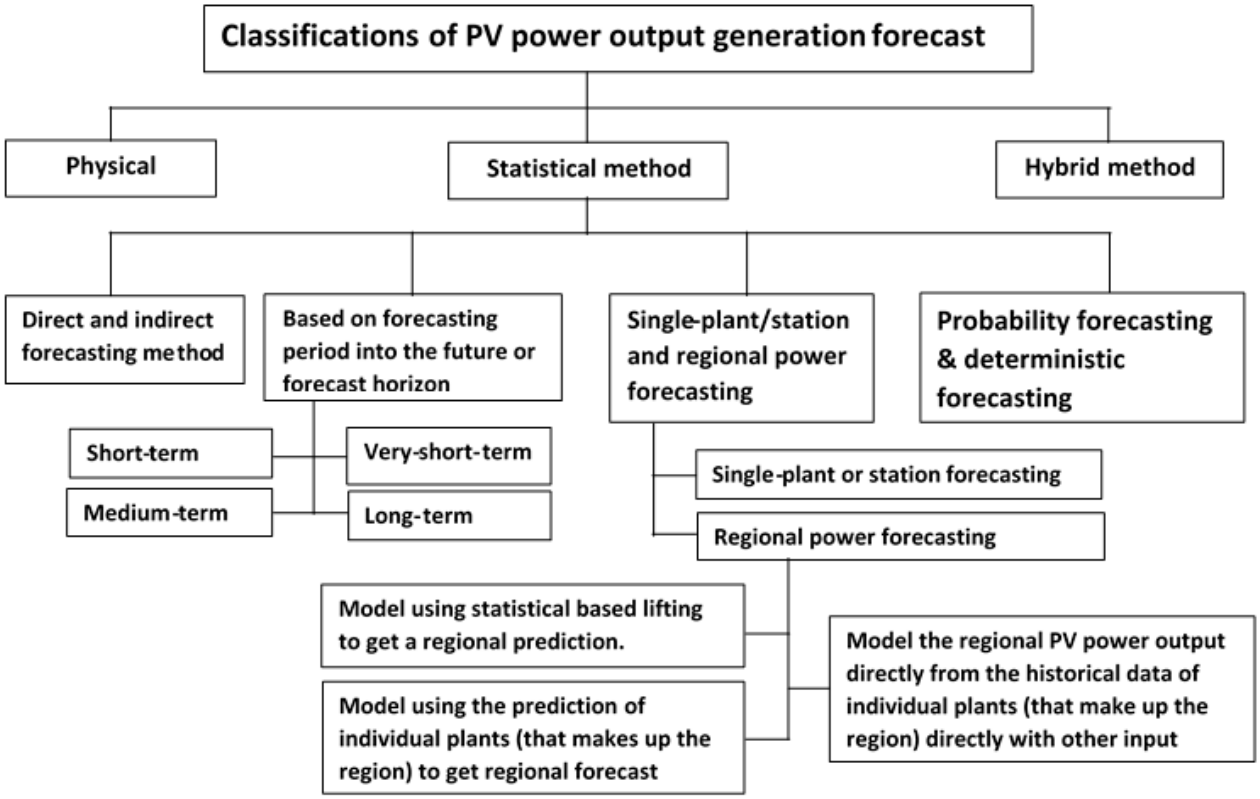

Figure 1. Classification of PV output power forecasting methods.

2.1. Physical Approach

This method simulates the conversion of solar irradiation to electricity using physical weather parameters, such as cloud coverage, ambient temperature, solar irradiance, etc., as the input vector into physical equations that forecast the power output. Physical models are designed using information about a specific site or location, weather parameters, panel orientation, and historical data. Models designed using this technique are simple when designed using global solar irradiance, but gradually become more complicated by adding other weather parameters (such as coverage, ambient temperature etc.) [12]. The technique is majorly affected by sudden high changes in weather variables. The physical model achieves higher accuracy with stable weather [10–14]. The numerical weather prediction

(NWP) model [15], total sky imagers (TSI) [16] and satellite images are some instances of physical method implementations [17].

One example of the physical approach is the image method. It makes predictions by analyzing the surface solar irradiance (SSI) of retrieved images from geostationary (meteorological) satellites. The cloud-index method is one common approach used to analyze and generate models from SSI data. The method compares satellite reflectance images with the corresponding ground albedo images, as well as basic cloud reflectance, to generate a cloud index, n. The relationship between n-th cloud-index and clear-sky index Kc is defined as the ratio of the global horizontal irradiance (GHI) to the concomitant modeled GHI under the sky no cloud condition. This relationship relies on an empirical decreasing function such as $Kc = 1 - n$ (in the simplest linear form). The GHI is the product of this clear-sky index, and an empirical (or theoretical) model or database of clear-sky irradiance [15,16]. Transforming SSI to a solar power-predicting model generally follows three steps. The first is transposing (or separating) the GHI into diffuse horizontal irradiance (DHI) and direct normal irradiance (DNI). The second step is to compute the global tilted irradiance (GTI) of the PV modules (also called the plane-of-array irradiance (POAI)). The third is to model the PV output power using the POAI. Two major methods can be applied for satellite-based forecasting of PV output power, relying only on temporal information and on both spatial and temporal (spatiotemporal) information [17–19].

2.1.1. Forecasting Approach Based on Temporal Information

Years of accumulated SSI images of locations or regions within the field of view of a geostationary satellite can be used to forecast PV output power for the locations, using statistical models together with the time series of irradiance data. The persistence (clear-sky index-based and smart persistence) methods [20] have used temporal information to model and forecast PV output power. The autoregressive models (AR), autoregressive moving average (ARMA) and autoregressive integrated moving average (ARIMA) [21], artificial neural network (ANN) [22], and k-nearest-neighbor (k-NN) [17,20] have also been applied, relying only on temporal information to forecast PV output power. These methods can be generalized mathematically as:

$$\widehat{Kc}(p, k + dk|k) = F\left(Kc^{sat}(p,k),\ Kc^{sat}(p,k-1),\ \ldots\right), \tag{1}$$

where $\widehat{Kc}(p, k + dk|k)$ is the model-predicted clear-sky index at location p, at a given time k, for the forecast horizon dk. The time is integer-indexed with respect to the SSI image (data) capture time. This predicted clear-sky index time is computed from a series of past lagged (or historical) clear-sky indexes $Kc^{sat}(p,k),\ Kc^{sat}(p,k-1),\ \ldots$ from the SSI database for the issue time k, for location p. The function F is obtained earlier from persistence or k-NN methods or earlier training periods from autoregressive or ANN models. Clear-sky-based persistence predictions are commonly used as a benchmark for other, more complex forecast methods, particularly for short-term forecasts.

2.1.2. Forecasting Approach Based on Spatial and Temporal Information

Geostationary satellites provide almost real-time long-term time series data for all locations in its field of view for the time series kilometric maps of SSI. A combination of spatial and temporal information can be explored by different methods to forecast PV output power. Some of these approaches analyze cloud motion vectors, while others rely on using statistical methods to model the spatiotemporal variability of the data.

A forecast based on the cloud motion vector (CMV) analysis starts by predicting solar radiation using time series images of geostationary satellites. It is often recommended for a forecast horizon between 1 to 5 h [21–26]. This method works by determining cloud vectors based on the analysis of consecutive satellite images. If the image features do not change significantly over a short interval, CMVs are computed using pattern-matching, or optical-flow methods are applied to successive images. The future cloud condition is approximated by extrapolating its motion, assuming the cloud speed, size, and shape, and

its optical properties persist [27]. The CMV-based PV output power forecasting method can be represented mathematically as [17]:

$$\widehat{Kc^{\mathrm{CMB}}}(p, k+dk|k) = Kc^{sat}(p - dk.dp(p,\ k), k), \tag{2}$$

where $\widehat{Kc^{\mathrm{CMB}}}$ is the CMV-based prediction of the clear-sky index at location p, at time k, for the forecast horizon dk. This predicted cloud-index is obtained using the clear-sky index, $Kc^{sat}(p - dk.dp(p,\ k), k)$, from the database (generated by the satellite at time k for a location p for the corresponding estimated CMV $dp(p,\ k)$ for a linearly extrapolated time dk. This implies that the CMV approach attempts to capture local fluctuations which already exist, directly and solely, in the clouds.

Dambreville et al. [21] proposed the statistical autoregressive modeling of spatiotemporal variability of the satellite image data for forecasting PV output power for a short-term horizon (of 15 to 150 min). This method accounts for past lagged clear-sky indexes of a set $Q(p)$ of the pixels surrounding the *p-th* location provided by the satellite-generated database $\left\{Kc^{sat}(p,k),\ Kc^{sat}(p,k-1),\ \ldots\right\}_{q\in Q(p)}$. Banc et al. [18] suggested integrating the autoregressive model with the past lagged clear-sky indexes, $\{Kc(k),\ Kc(k-1), \ldots\}$, which were obtained from measurement. The predicted spatiotemporal autoregressive clear-sky index for location p, at time k, for forecast horizon dk, is given as:

$$\widehat{Kc^{\mathrm{AR_{st}}}}(p, k+dk|k) = \alpha_0 + \sum_{\substack{q\ \in\ Q(p) \\ 0\ <\ l\ <\ L}} \alpha_{ql} Kc^{sat}(p, k-1) + \sum_{0<n<N} \beta_n K_c(k-1) \tag{3}$$

where $\{\alpha_0\}$, $\left\{\alpha_{ql}\right\}$ and $\{\beta_n\}$ are the autoregressive parameters determined by training for the target period with the historical data in an optimal manner, by reducing the RMSE for dk. They concluded saying that using the spatiotemporal information in the vicinity of the target location improved the autoregressive forecast performance by 19%, with respect to RMSE.

2.2. Statistical Technique

Statistical techniques are mostly developed from the principle of persistence or random time series. Solar PV output power predicting models are developed by determining the relationship between the input variables (vectors) and corresponding output power using validated standard/scientific procedures. The weather parameters (cloud coverage, temperature, rain, wind, humidity, module temperature etc.) which affected the solar PV output power that was used as input data for the forecasting algorithm are referred to herein as the input variables or vectors. Some examples of techniques used under this category are traditional statistical analysis and artificial intelligence (AI), or machine learning (ML), analytics. The traditional forecasting approaches [28] apply regression analysis techniques to the time series data to produce models that forecast PV output power. Some examples of AI forecasting techniques are artificial neural networks (ANN) [26,27], support vector machine (SVM) [26,28], long short-term memory (LSTM) [6,29,30], etc. It should be noted that various modifications of the mentioned AI techniques are also applied.

Owing to the advancement in measurement techniques that generate large amounts of data over the years, commensurate advancement has also been made in the data modeling technologies that consume these data. The following subsections provide an overview of the four statistical forecasting approaches shown in Figure 1.

2.2.1. Direct and Indirect Forecasting Models

Direct forecasting models use historical PV output data samples to make predictions [31]. Direct forecasting models attempt to determine the relationship between the input variables and PV output power by analyzing historical data. Indirect forecasting techniques follow two steps [32,33]. In the first step, the weather factors that affect solar

PV output power, such as solar irradiation, are modeled, while the second step transforms the result of the first step into predicted PV output power [8,31]. The major difference between these two techniques is that the direct method does not need the value of the solar irradiance to be calculated at an intermediate stage. Image-based, numerical weather prediction (NWP), artificial neural network (ANN), and hybrid ANN have used indirect forecasting methods on different time scales to forecast solar PV output power [34–44]. Many commercial PV output power simulation software, such as PVSol [45], PVsyst [46], PVGIS, PVWatts and RETScreen [15], and Helioscope [47], have used these methods to forecast PV power generation. These software applications use the forecasted solar irradiance and related weather (environmental) data as input for their predictions. They have implemented direct and indirect methods to forecast the next-day power generation of a PV system, and showed that the direct method is the better of the two. Gandoman et al. [48] reviewed the literature on short-term forecasting of solar PV output power based on cloud cover influence. The indirect methods provide a more accurate forecast, as they consider site-specific losses before predicting energy yield values.

2.2.2. Classification of PV Power Forecasting Based on the Forecast Horizon

The forecast horizon is the length of time into the future for which the PV power output forecast is being made. The forecast accuracy varies with the forecast period into the future using identical model parameters. Hence, one should consider the forecast horizon when designing a model. Based on the forecast horizon, the PV output power generation forecast can be subcategorized into four types—very short-term forecast, short-term forecast, medium-term forecast, and long-term forecast horizons. Very short-term forecasting is when the forecast horizon is a few seconds to one minute, but less than one hour. A short-term forecast is considered to be when the PV power generation forecast is conducted for a period from one day to several days. The short-term forecast ensures commitment, scheduling, and dispatch of generated electrical power. It also enhances the security of the power grid operation. The medium-term forecast is the category that is conducted for a period of one week to one month. This category smooths the planning of the power system and maintenance schedule by forecasting the power availability in the future. When the PV power forecast horizon is from one month to one year, we consider it a long-term forecast. This category is vital to electricity generation, planning, transmission, and distribution. Table 1 summarizes the PV output power forecast classification based on the event horizon. Although we have considered the forecast horizon as a subclass of statistical method, every forecasting technique is used to forecast PV output power for some period into the future; hence, they all belong to this category.

Table 1. Summary of classification of PV power forecast based on the forecast horizon.

Forecast Horizon	Time/Period	Application/Benefits
Very short-term	<1 min	Controlling power distribution
Short-term	1–many hours	Ensures commitment, scheduling, and dispatch
Medium-term	1 week–1 month	Smooths the planning of power system and maintenance schedule
Long-term	1 month–1 year	Helpful for power generation transmission and distribution

2.2.3. Single Plant and Regional Power Forecasting

The electrical power produced by several solar PV power plants or stations can be combined to form a regional grid. When a forecasting model is designed to predict the PV output power of a single station, we consider it a single plant or station power forecasting. Regional PV output power forecasting is when the prediction is for a group of stations under the same administrative region or area.

Regional forecasting has been investigated in three ways:

- Summation of the results (or predictions) produced by the models of the individual stations that make up the region or area to make a prediction [49].
- Statistical scaled-based lifting of the prediction from the individual plants (or stations) that make up the region [45,46].
- Modeling the PV output power for the region using combined historical data of the individual stations that make up the region.

2.2.4. Probabilistic and Deterministic Forecasting Methods

PV output power forecasting methods can be categorized as probabilistic or deterministic [29]. The probabilistic approach attempts to approximate the probability of all possible results of the solar PV output power, while the deterministic approach makes a forecast of the PV output power into the future without considering the forecast uncertainties. The former produces an unambiguous estimate of the PV output power prediction and gives the prediction's margin of error. It provides more detailed information about its forecast compared to the deterministic method [47–49].

2.3. Hybrid Method

The hybrid technique combines physical and statistical techniques to make predictions. The physical model given by the manufacturers for the PV modules is first applied, and then a statistical approach is used on the result to improve accuracy. Combining two different physical or statistical techniques is also a form of hybrid. Studies [47–50] have combined the physical forecasting technique with other artificial intelligence and statistical techniques to achieve higher accuracy. They combined ANN and physical methods to formulate a physical-ANN hybrid (PHANN). The work simulated a theoretical model of the sky (for a location)—by simulating solar irradiation for a sky with no clouds (using the clear sky solar radiation model)—and used this simulated irradiation to set the optimal daytime limit. Hence, PHANN optimizes the features of the two methods. One drawback of the hybrid method is that it becomes more complex because it involves more than one technique and consumes relatively more machine resources.

3. Data Analytics

This section investigates the data analytic procedures applied for power forecasting under the different approaches highlighted in Section 2. Generally, energy data analytics are carried out in three stages. We have the pre-processing of raw input data, the algorithm and modeling stage, and then the evaluation of the accuracy of the estimates.

3.1. Input Data

Solar energy is one of the most popular renewable energy sources, which comes from the sun in the form of solar irradiance. Solar cells are made up of materials which convert solar irradiance to electricity through the photovoltaic effect. PV power generation mainly depends on the amount of solar irradiance. In addition, other weather parameters, including atmospheric temperature, module temperature, wind speed and direction, and humidity, are considered potential parameters for estimating the PV output power. There are also power losses due to soiling and degradation of the PV module and its electronic components. A significant number of historical time series data of PV output power and corresponding meteorological variables are used to establish the forecasting model of PV power generation. The historical time series data are normally divided into two groups: the training and testing data. About 70–80% of the data is reserved for training (or learning) by the model, while 30–20% is reserved for testing and validating the PV power forecasting model.

Meteorological parameters change with location and weather conditions; hence, their effects on PV power generation differ at different geographical locations. This fact notwithstanding, a forecasting model's performance depends on the correlation of the model's input parameters and output values. The correlation between meteorological input data,

such as atmospheric temperature, solar irradiance, wind speed and direction, and module temperature and humidity, and output power should be considered. The strongly correlated input variables should be taken as input vectors for the forecasting model, while the weakly correlated ones may be discarded. Studies, such as [51], have shown that solar irradiance strongly correlates with output power, and must be used as one of the input vectors in developing PV power forecasting models. One should study the correlation between other meteorological variables with PV output power before designing a PV output power forecasting model. The higher the number of variables used as input vectors, the higher the accuracy of the forecasting model, but the higher the complexity and computational cost of the model. One must find the optimum number of input vectors based on correlation, (selecting only those which are of the utmost importance) to achieve high accuracy and with minimum computational cost.

Historical data used for direct PV output power forecasting may sometimes have spikes or nonstationary components due to changing and uncertain weather conditions [50,52–54]. Components considered to be outliers will give rise to high forecast errors. Additionally, missing input data points from measurement errors or other errors will also increase the forecasting errors of the model. Therefore, there is a need for pre-processing of input data. Improper training problems and computational costs can be significantly reduced by pre-processing the input data, thus improving the forecasting (predicting) models' accuracy.

Many techniques have been used to pre-process input data of forecasting models, one of which is the wavelet transform (WT) [55]. Solar PV time series data often have spikes and different kinds of nonstationary behavior. WT can be used to pre-process the input data in order to improve solar PV output power model forecast errors. The continuous wavelet transform (CWT) and discrete wavelet transform (DWT) are two classes of WT. The CWT can be expressed mathematically as [56]:

$$\mathrm{CWT_x}(a,b) = \frac{1}{\sqrt{|a|}} \int_{-\infty}^{+\infty} \Psi^*(t)x(t)dt,\ a > 0 \tag{4}$$

$$\Psi(a,b) = \frac{1}{\sqrt{|a|}} \Psi \frac{t-b}{a},\ a > 0,\ \text{and} - \infty < b < +\infty \tag{5}$$

where $x(t)$ represents the time series signal, $\Psi_{a,b}(t)$, is the mother wavelet scaled by a factor and shifted by a translated parameter b, and * denotes complex conjugate. High-frequency (low-scale) variations compress the signal and produce detailed information concerning it, while low frequencies (large-scale) variations expand the signal and give non-detailed information about it. CWT is obtained by continuously scaling and translating the mother wavelet to generate meaningful redundant information [57]. Hence, the mother wavelet is scaled and translated with some scales and position information, referred to as DWT. DWT uses the position and scale values that rely on the power of two, known as dyadic translations and dilations. These are obtained by discretizing the scaling and translation parameters, given as [56]:

$$\mathrm{CWT_x}(m,n) = 2^{-\frac{m}{2}} \sum_{t=0}^{T-1} x(t)\Psi\left(\frac{t-n.2^m}{2^m}\right), \tag{6}$$

where T represents the length of the signal $x(t)$. The translation and scaling parameters are functions of the integer variables m and n. The variables $a = 2^m$, $b = n.2^m$, and t represent the discrete time series index. WT decomposition processes data by filtering (low-pass and high-pass filters) and down-sampling, while reconstructing involves up-sampling and filtering.

Normalization is a commonly used technique [55–57] for pre-processing input data to produce PV output power forecasting models. This typically reduces a wide range of input data values to a smaller range to decrease regression errors and improve accuracy. Data can be restricted to fall between 0 and 1, using:

$$P_{\text{Normalised}} = \frac{P_{\text{actual}} - P_{\text{min}}}{P_{\text{max}} - P_{\text{min}}}, \tag{7}$$

where $P_{\text{Normalised}}$ is the normalized data, P_{actual} is the measured data, while P_{max} and P_{min} are the maximum and minimum measured data, respectively.

Other examples of pre-processing techniques include trend-free time series [58], self-organizing map (SOM), stationary, historical lag identification [59], and normalization [60]. If pre-processing was performed on the input data, then post-processing must also be applied to the output using the appropriate post-processing technique before analyzing the performance of the PV output power forecasting model.

3.2. Forecasting Models and Algorithms

We will consider some selected solar PV output power forecasting methods in this section. These methods include persistence, statistical, machine learning, and hybrid approaches.

The persistence model involves the use of the solar PV output of the previous day at the same time. The method requires only the historical solar PV output power for the forecasts. The model is often used as a benchmark for other techniques, as well as for short-term PV output power generation forecasting. The method involves applying statistical tools to analyze the different input variables for forecasting PV output power. Hence, historical time-series data are used in this method [61]. There is also the need to ensure that very recent data are included in the analysis for higher accuracy. The machine-learning (ML) technique is a smart tool for modeling linear, nonlinear, and non-stationary data trends. It should be noted that the ML technique requires a large amount of input data for increased accuracy.

ML and other AI techniques depend largely on statistical methods. A few of the widely applied statistical tools are discussed in the following subsections.

3.2.1. The Persistence Model

The persistence model is often considered a fundamental and standardized statistical method. It is, therefore, usually applied to compare the performance of other forecasting models to evaluate their accuracy. In the persistence model, the value of the PV output power is assumed to be the same at the same time for the previous or the next day. This technique is commonly used for short-term forecasting, particularly hour-ahead forecasting of solar PV and wind energy output power. This model's accuracy depends on the weather's stability, and as the forecast horizon increases, so do the forecasted power errors [61]. The naïve and smart persistence approaches are some implementations of the persistence model (to mention a few).

The naïve persistence model assumes that the predicted PV power is the same as the measured power on the previous day, for the same time, as:

$$P_n\ (T + h) = P_{pd}(T). \tag{8}$$

It is commonly used for very short-time forecast horizon and stationary time series PV data. The solar PV output power time series data are non-stationary, so this technique splits the PV power production into stationary and stochastic patterns. The stationary portion is applied on clear-sky days, while the stochastic is applied on cloudy days, which affects PV output power production [62].

Another type of persistence model is the smart persistence model. This technique is commonly used to model nonstationary time series PV data, and is expressed mathematically as [62]:

$$P_i(T + h) = \begin{cases} P_{nc}(T + h), \text{ if } P_{nc}(T) = 0, \\ P_{nc}(T + h)\frac{P}{P_{nc}(T)}, \quad \text{otherwise} \end{cases}, \tag{9}$$

$P_{nc}(T)$ is the predicted power during a clear sky. $P_{nc}(T)$ is very accurate for the short-term forecast horizon for the period when the data have low variability [23]. This prediction

technique has two parts—the stochastic and clear-sky PV output power prediction—as can be seen in Equations (10) and (11) [62].

$$P\,(T) = P_{nc}(T) + P_{nl}(T+h) \tag{10}$$

$$P_i(T+h) = P_{nc}(T+h) + P_{nl}(T) \tag{11}$$

where $P_{nl}(T)$ is the stochastic term.

3.2.2. Autoregressive Moving Average Technique

The autoregressive moving average (ARMA) model is a statistical technique or tool that combines the autoregressive (AR) and moving average (MA) techniques. The ARMA model is expressed mathematically as [63]:

$$X(t) = \sum_{i=1}^{p} \alpha_i X(t-i) + \sum_{j=i}^{q} \beta_j\, e(t-j), \tag{12}$$

where $X(t)$ is the forecasted PV output power; p and q are the order of α_i and β_j coefficients, respectively; and $e(t)$ represents the white noise that produces random uncorrelated variables with a zero average and constant variance [64]. The popularity of the ARMA model comes from its ability to extract statistical properties and its adoption of the Box–Jenkins method [65]. AR-integrated MA (ARIMA) is a widely used extension of this model for PV output power forecasting with proven accuracy [66]. The integrated portion removes any form of non-stationary characteristics in the data [67]. The technique can be used independently or as a hybrid with other forecasting models to forecast PV output power [25]. One can use the regression method to establish a relationship between the exploratory variables (weather parameters) and dependent variables (forecasted PV output power).

3.2.3. Regression Technique and Exponential Smoothing Technique

Oudjana et al. [68] applied simple and multiple regression models to forecast PV output power. They fed the regression models both solar irradiance and temperature as input variables to produce higher accuracy than when they were used separately. One shortcoming of this technique was that it required the design of a mathematical model and many explanatory variables to use it.

Ostertagova and Ostertag [69] introduced the simple exponential smoothing method. This method performs well with stationary data without a time-series trend, such as MA. Holt improved this technique to produce Holt's method [70], while Winter modified Holt's method to produce the Holt–Winter method [71]. This approach allows unequal weights to be applied to the historical data where the applied weights decay exponentially – recent past to distant past times. The simple exponential technique has been implemented in exponential weighted MA (EWMA), which can be expressed mathematically as [72]:

$$\overline{X}_{l+1} = \alpha X_l + (1-\alpha)\overline{X}_l = \overline{X}_l + \alpha\left(X_l + \overline{X}_l\right), \tag{13}$$

where α is the smoothing constant and takes any value between 0 and 1. EWMA needs an initial forecasted or assumed value, which can be, for example, $\overline{X}_{l+1} = \alpha X_l$. The model indicates that the forecasted value at time $l+1$ equals the summation of the last forecasted value, $\overline{X}_{l+1}$, and the error adjustment in the forecast is $\alpha\left(X_l + \overline{X}_l\right)$. If a trend exists in the data, the EWMA forecast will lag behind [9].

3.2.4. The Artificial Neural Network

Artificial neural network (ANN) is yet another statistical model which is considered the most effective and popular machine learning algorithm used in modeling and forecasting PV output power, because it can handle the non-linear relationship between the input meteorological data and the output PV power. It has been shown to have a high success rate in predicting PV output power [70–74].

It is better suited to handling the nonlinear and complex relationship between the input features (meteorological data) and the solar PV output power without any prior assumption. Figure 2a shows the basic components of an ANN—the input, hidden and output layers, neurons, and connections. Different input data are fed into the input layer. The hidden layer could have one or more layers for data analysis. The output layer completes the data processing to provide the network output, while the connections link up the different neurons in adjacent layers, together with the updated weights [75]. Figure 2b gives a pictorial representation of a basic ANN cell. This figure shows that a neuron cell has two main components—the combination and activation functions. The combination function performs a summation of all input values. This network produces a result by performing a weighted sum of the inputs using the activation function. Hence, the activation function behaves as a squeezing function to transfer the input to the output. Linear, Gaussian radial basis, sigmoid, hyperbolic tangent sigmoid, bipolar step, bipolar linear, unipolar step, unipolar, and linear functions are some of the commonly used activation functions in ANN. An ANN can be expressed mathematically as [76]:

$$U_J = b + \sum_{k=1}^{J} (W_k \times I_k), \tag{14}$$

where U_J is the final network output, b is the bias weight, J, W_k, and I_k are the number of inputs, connection weight, and network input, respectively.

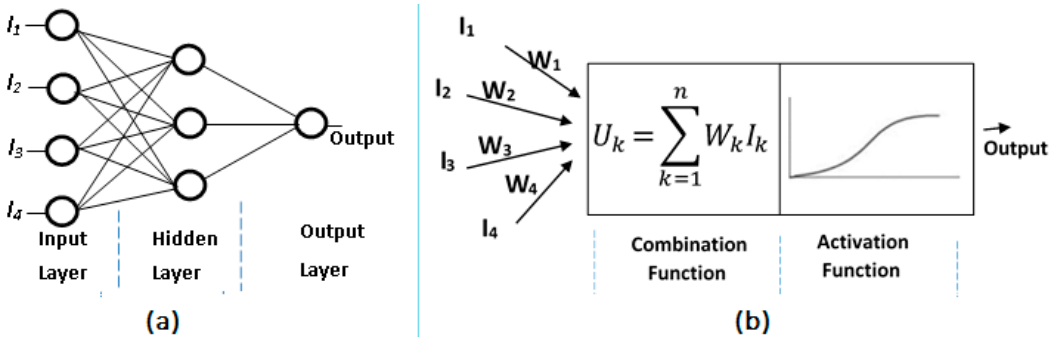

Figure 2. (**a**) Schematic representation of an ANN with the input, hidden and output layers. (**b**) A pictorial presentation of a mathematical model of an ANN cell [75].

Training and testing are two basic steps of a neural network. The training phase involves training the network and learning algorithm, with some part of the input data reserved for training. The neural network learning algorithm tries to find a mapping relationship by updating the synaptic weight values. Errors are then calculated by comparing the output results with the expected or actual measured data. The inference drawn from the magnitude of the error values is used to update the weights and biases. This process is repeated until the desired degree of accuracy is obtained. Hence, the NN at the training step produces the desired result using the test input dataset and the model weights. The final output result of the NN changes with changes in the network architecture used, activation functions, and network input. Some of the commonly used activation functions for PV output power generation forecast include, but are not limited to, sigmoid, Gaussian radial basis, and hyperbolic tangent sigmoid functions. This is because they are differentiable continuous functions that can handle non-linear relationships in the NN [77].

Oftentimes, NNs with a single layer have been employed to solve PV power forecasting problems, but for complex nonlinear patterns between the input data set and expected output result, single-layer NNs develop unsolvable issues. Multilayer NNs have been developed, which employ different architectures and data mapping algorithms to handle complex cases, with a non-linear relationship between input and output data. Some of the commonly used multilayer NNs are radial basis function neural networks (RBFNN),

multilayer perception neural networks (MPLNN), adaptive neuro-fuzzy interface systems (ANFIS), multilayer feedforward neural networks (MLFFNN), general regression neural network (GRNN), and recurrent neural network (RNN).

MLPNN is a type of feedforward supervised ANN which may have more than one hidden layer between its input and output layers [78]. The number of hidden units one uses in the NN depends on the complexity of the problem. Zhang et al. [79] have demonstrated that more than two hidden layers are rarely needed for the NN to carry out complex input-to-output mapping. PLPNN has been used to forecast PV power generation in the past. It has also been applied to electricity and price forecasting [80]. MLFFNN is another NN architecture which works by moving information from the input to the output in one direction—forward only. It was the first ANN to be implemented, and it is simpler than the other ANNs. It does not employ a feedback loop while processing data. Forecasting and pattern recognition are some of the many areas in which this NN has found applications [81]. Gupta et al. [82] categorized RBFNN as a two-layer NN. Its learning phase is divided into two stages depending on the synaptic weights used. Performance analysis conducted by [83] demonstrated that RBFNN takes less computational time to learn the features in the data and to obtain good results. They also can easily produce a generic model and have a strong tolerance for input noise. RBNN is often a common choice for PV output power forecasting because of its structural simplicity and universal approximation attributes [84]. RNN shows good performance when learning the different complex relationships between the NNs input and output data, and, hence, it is deemed a suitable tool for time-series PV output power forecasting [85]. output PV power forecast results produced using RNN have significantly reduced errors compared to that of FFNN [39]. GRNN is a type of probabilistic-based NN that performs more regression than task classification [86]. This network has strong nonlinear mapping capability, and can handle nonlinear mapping problems. It is a fast-learning algorithm, and is easy to tune. One weakness of this NN is that its computation power requirement grows with the size of the method, and the selection of the parameter σ is important when using it [55]. One of the most powerful supervised ML algorithms is the backpropagation (BP) algorithm [87], but this has the weakness of easily falling into a local minimum, its convergence rate is slow, and its training process is prone to oscillations [88]. To harness the benefits of the NN, Ref. [89] introduced a modified BP network to handle some of these weaknesses. The BP neural network (BPNN) has been the popular NN choice because of its excellent nonlinear mapping function, which is perfect for solving complex regression problems [90].

One type of adaptive multilayer feedforward NN is the ANFIS. This model can have both linguistic and numerical knowledge of the data, and could be able to classify and identify patterns in the data. It is more transparent to the user and has fewer memory errors than ANNs [91]. It has been used to carry out nonlinear forecasting, where past samples are used to make forecasts in advance [92]. One needs to tune the member functions of ANFIS to improve its performance [56]. It is the most commonly used fuzzy network because it is transparent, has a low computational cost, and produces robust results comparable to those of the statistical models [93] (more comprehensive information on different NNs can be found in [94]). The benefits of NNs notwithstanding, one disadvantage they have is their requirement for a large input training dataset and the issue of overfitting [9,92,95].

3.2.5. Support Vector Machine

Another supervised ML method is the support vector machine (SVM). It is founded on the structural risk minimization (SVM) principle [96]. This principle works by minimizing the upper bound of the expected risk. Hence, the SVM technique minimizes the errors in the input training data. Vapnik [97] created the SVM to tackle classification tasks, but this technique was lately modified to solve regression problems, known as support vector regression (SVR). PV power forecasting is a typical problem that can be implemented with SVR [98]. The SVR algorithm works by mapping the (non-linear) input time series data into a higher-dimensional space through non-linear mapping before performing linear regres-

sion in the new space. Assuming we have a set of training data, $\{(x_1, y_1), \ldots, (x_k, y_k)\}$, where $x_k \in R^n$ are weather parameters (input vector) and $y_k \in R^n$ are the corresponding PV output power, the modeling function $f(x)$ is given as [37]:

$$f(x) = w \times \psi(x) + b, \tag{15}$$

where $\psi(x)$ is the input vector, $w \in R^n$ is the weight vector, and $b \in R^n$ is the bias term that is approximated by minimizing the regularized risk function, given as [96,97]:

$$R(C) = C\frac{1}{N}\sum_{i=1}^{N} L_{\in}(y_i, f_i), + \frac{1}{2}||\ W||^2, \tag{16}$$

where $L_{\in}(y_i, f_i) = \begin{cases} |y_i - f_i|, \text{ if } |y_i - f_i| \geq \in \\ 0, \text{ otherwise} \end{cases}$ is the ϵ-insensitive loss function, C and ϵ are the user-determined prescribed parameters, y_i represents the measured value, and f_i represents the prediction value at period i. When the forecasted value is within the ε-tube in Figure 3, we have zero losses, while ξ is the distance between the data and corresponding ε-tube boundary values. The term $\frac{1}{2}||W||^2$ evaluates the flatness of the function.

The performance of SVR depends very much on the choice of kernel function and its parameters [60]. The linear, polynomial, Gaussian RBF, and sigmoid functions are instances of frequently used kernel functions for SVR. The linear kernel function is represented mathematically as:

$$z(x_j, x_k) = x_j^T x_{k.} \tag{17}$$

This kernel is used when the variation in the data is small [99–104]. The polynomial kernel is expressed mathematically as:

$$z(x_j, x_k) = (\gamma x_j^T x_k + r)^d, \ \gamma > 0, \tag{18}$$

where r, d and γ are parameters of the kernel. d represents the degree of the polynomial; it represents the training data in feature space [99–104]. The Gaussian RBF is expressed mathematically as:

$$z(x_j, x_k) = \exp\left(\frac{||x_j - x_k||^2}{2\sigma^2}\right) = \exp(-\gamma||x_j^T - x_k||^2, \ \gamma > 0, \tag{19}$$

where $\gamma = \frac{1}{2\sigma^2}$ is a constant that moderates the RBF width. This kernel is applied in infinite dimensional space. The sigmoid kernel function is expressed mathematically as:

$$z(x_j, x_k) = \tanh\left(\gamma x_j^T x_k + r\right), \tag{20}$$

where r and Υ are kernel parameters, r is the shift parameter which controls the threshold of mapping, and x_j and x_k in Equations (17)–(20), respectively, represent the inner vectors in $\varphi(x_j)$ and $\varphi(x_k)$ feature spaces.

Cherkassky and Ma et al. [105] demonstrated that three parameters dominate the performance of the SVR-based model used for forecasting PV output power. One of the parameters is the penalty (C). This determines the penalty for error estimation. ϵ, the tube radius, states the data inside the tube that can be ignored during regression. The third is the kernel function parameter. The performance of the SVR depends heavily on the choice of these three parameters. The choice of C, ϵ, and kernel function parameters should be carefully selected to develop a good forecasting model. This dependence of the performance of the SVR on the selection of these parameters is a limitation to this.

Most models' forecasting ability and performance do not meet one's expectations. This is expected, because every model is often limited to its definition of the analytic challenge to be resolved. Combining two or more modeling techniques—known as the hybrid technique—can leverage the advantages of each method and make up for its limitations.

The hybrid modeling technique has been used to achieve high accuracy for different PV power generation forecasting techniques. This method can produce better performance and accuracy if carefully designed to harness the component technique's merits, rather than as a stand-alone method. Yona et al. [106] successfully implemented the Fuzzy inference model together with RNN for PV power generation forecasting. The fuzzy inference technique was first used to smooth out the meteorological input data before feeding it into the RNN for the PV power generation forecast. Chen et al. [107] demonstrated that the hybrid fuzzy-GA forecasting model gave a good performance for PV power generation forecasting. The wavelet transform (WT) technique is often used in combination with different ANNs, where it is first used to de-noise the input data before feeding the result into the ANN. Colak and Qahwaji [108] used a hybrid model of WT and SVM, where they de-noised the meteorological data with WT before passing it into the SVM method for PV power generation forecasting, which minimized the prediction errors. The hybrid method, which combines two or more modeling techniques, increases this technique's complexity and computational cost compared to that of the individual techniques. This technique's accuracy is affected by the choice of a single technique with poor performance. If one of the component techniques in the hybrid shows poor performance, it affects the overall performance of the hybrid. This is one limitation of this method.

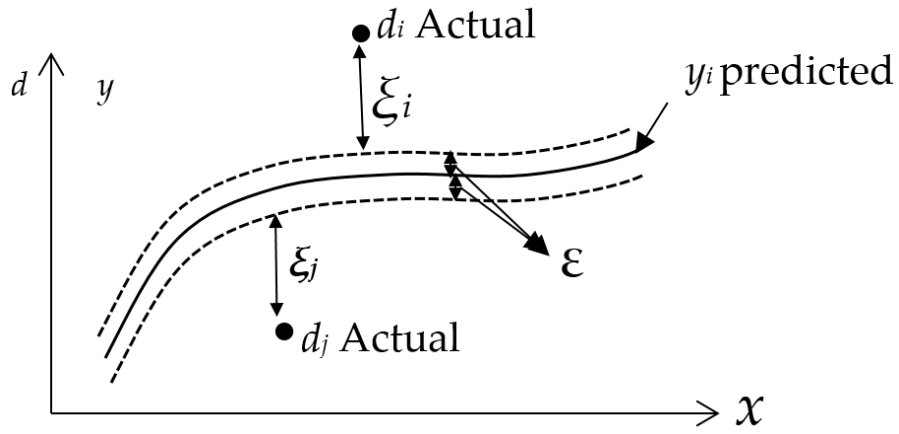

Figure 3. Parameters of SVM [101].

3.2.6. Deep Learning Neural Networks

The deep learning neural network algorithms are one AI technique consisting of a multilayer perception NN. It uses multiple layers to capture the nonlinear behavior between the input features and output values. It has been applied in medical diagnosis (e.g., to predict tumors), wind turbine fault detection, etc., and could be applied for solar PV and wind energy power output generation forecasting. One of the advantages of this technique is that it is very good at extracting useful information (data) from noisy data. Another is that it provides visual analytic graphs after the training phase to give deep insights into the data. It also offers the possibility of data discrimination, and can transform unstructured into structured data using convolutional neural networks (CNN) or deep belief methods. Many practical problems can be solved by following how the human brain works. One disadvantage of this technique is that it often requires supplementary machine resources such as GPUs or CPUs. They also have the problem of overfitting and hyperparameter optimization issues [105]. This technique suffers from under-fitting when the number of passes (iteration) is too few, and overfitting when the number of passes is too many. The sigmoid, tanh, Rectified Linear Unit (ReLU), and leaky ReLU are some of its commonly used activation functions [106–109].

3.2.7. Parameter Extraction of Solar PV Models

The characteristics of a PV system can be analyzed by considering the power-voltage (P-V) and current-voltage (I-V) curves. The shape of these curves depends on parameters

such as solar irradiance, ambient temperature, PV model equivalent circuit, and other unknown parameters [110–113]. The PV model equivalent circuit can be used to investigate the relationship between these parameters and the behavior of these curves [114]. There are three types of PV equivalent circuit models—single-diode model (SDM), double-diode model (DDM), and three-diode model (TDM) [115]. The number of unknown parameters associated with each model is five for the SDM, seven for the DDM, and nine for the TDM. The SDM is often seen as a reference model [116] and is the common choice due to its balance between having fewer (model) parameters and ease of implementation. The DDM is often called the seven-parameter model. Khanna et al. [117] mentioned that TDM is an appropriate platform, although it has a larger number of parameters and is more complex to implement.

Several techniques have been applied for PV model parameter extraction. These methods can be analytic or numerical. Analytic methods are identified by their ease of implementation, while sacrificing accuracy. To form I-V curves of the data, which will be used as input for the analytic method, depends on the manufacturers' datasheet for the open circuit voltage, short-circuit current, and maximum power values. This dependence is a disadvantage of this method because these data are usually unavailable for all environmental conditions or may be inaccurate. To solve this problem, researchers turned to numerical methods. In the numerical method, optimization algorithms depend mostly on an iterative approach to solve the problem of estimating the parameters. The numerical method can be divided into deterministic and metaheuristic methods. Deterministic methods easily fall into a local optimum if the case at hand has multiple local optima, because of their dependence on initial input values [118]. In contrast, the metaheuristic method does not depend on initial values [119].

These unknown parameters can be estimated using iterative methods, machine learning, or metaheuristic optimization algorithms [120–126]. Many metaheuristic methods have been used to extract PV model parameters. These include the Lambert W-function [127], the Gauss-Seidel [128], the ant lion optimizer (ALO) [129], the shuffled frog leaping algorithm [119], linear least squares [130], and maximum likelihood-based Newton–Raphson [131] are a few of the iterative methods which have been applied to estimate these parameters.

Parameter optimization for the DDM has successfully been accomplished using a biography-based optimization [132] algorithm, particle swarm optimizer (PSO) [133], salp swarm algorithm [134], cat swarm optimization [132], combined differential evolution/whale optimizer [135], improved shuffled complex evaluation model [136], a self-adaptive ensemble-based differential evolution algorithm [137], and an opposition-based learning modified salp swarm algorithm [138].

Recently, several metaheuristic optimization methods have been applied to extract these PV parameters, such as the multiple learning backtracking search algorithm [139], moth-flame algorithm (MFA), orthogonal Nelder–Mead [140], the elephant herd algorithm [141], logistic chaotic JAYA algorithm [142], opposition-based sine cosine approach with local search [143], gray wolf optimizer, teaching–learning-based optimization (TBLO), chaotic improved artificial bee colony (CIABC) [144], cuckoo search algorithm, etc. TBLO has been used [145] to estimate TDM parameters. MFA has been applied to estimate TDM parameters [146], assuming ideal conditions for the second and third diodes (as controlled variables). Many techniques which have been used to extract optimal PV model parameters can be found in the literature. However, a recently new optimization technique, known as the turbulent flow of water-based optimization (TFWO) [147] method, has designed extract parameters for the three types of PV cells [115]. The gorilla troops optimization (GTO) algorithm [148] is yet another recent technique that has proven to be efficient in PV model parameter optimization, because it has only a few parameters to adjust, and is easy to implement. The supply–demand optimization (SDO) algorithm is another optimization technique which has been used to optimize parameters for the solar PV model. SDO, like the GTO, is simple to implement and has few parameters to be adjusted [149]. The

heap-based algorithm (HBA) is yet another recent [150] technique that has been used to extract optimal parameters for the PV model. Later in this subsection, we will provide a detailed explanation of the TFWO and GTO algorithms.

Figure 4 presents the SDM equivalent circuit diagram for a PV solar cell, and the output current is computed mathematically as [115]:

$$I = I_{\text{ph}} - I_{\text{d1}} - I_{\text{sh}}, \tag{21}$$

$$I = I_{\text{ph}} - I_{\text{s1}}\left[e^{\frac{q(V+IR_s)}{a_1 KT_c}} - 1\right] - \frac{V + IR_s}{R_s}, \tag{22}$$

where the photo-generated current is I_{ph}, the leakage current in the PN junction is I_{sh}, the shunt resistance is R_{sh}, I_{d1} represents dark saturation current, R_s, represents the series resistance, the ideal factor of the diode is a_1, K represents the Boltzmann's constant, q represents the charge of the electron, and T_{c} represents the PV cell temperature.

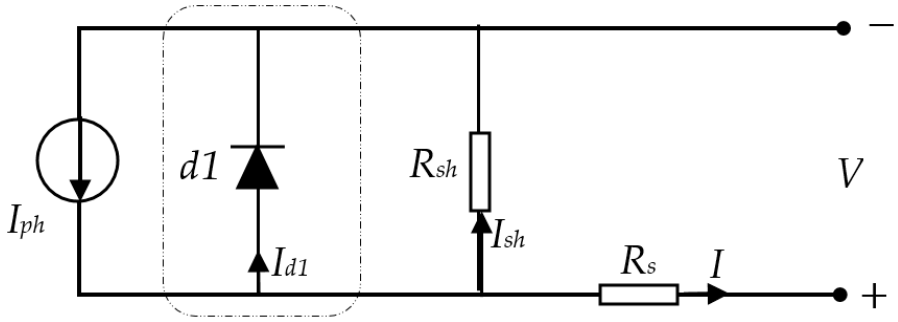

Figure 4. SDM equivalent circuit.

The five model parameters that need to be optimized for the SDM are $\left(I_{\text{ph}},\ I_{\text{s1}},\ a_1,\ R_{\text{s}},\ R_{\text{sh}}\right)$.

The DDM's equivalent circuit has a second diode added to the diode section (enclosed in a rectangle with dotted lines) of Figure 4. The output current is calculated with Equation (22), but with another term for the second diode added (which is of the form of the second term of this equation) to account for the new diode component. We then have two new parameters, I_{s2} and a_2, so the seven model parameters of the DDM model are $\left(I_{\text{ph}},\ I_{\text{s1}},\ a_1,\ R_{\text{s}},\ R_{\text{sh}},\ I_{\text{s2}},\ a_2\right)$. For the TDM model, a third diode is added to the equivalent circuit of Figure 4, and the equation to calculate the output current of the TDM has another term added for the third diode component. Hence, the nine model parameters of the TDM are $\left(I_{\text{ph}},\ I_{\text{s1}},\ a_1,\ R_{\text{s}},\ R_{\text{sh}},\ I_{\text{s2}},\ a_2,\ I_{\text{s3}},\ a_3\right)$. Below is a summary of the model parameters of the three PV models:

For SDM: $\left(I_{\text{ph}},\ I_{\text{s1}},\ a_1,\ R_{\text{s}},\ R_{\text{sh}}\right)$;

For DDM: $\left(I_{\text{ph}},\ I_{\text{s1}},\ a_1,\ R_{\text{s}},\ R_{\text{sh}},\ I_{\text{s2}},\ a_2\right)$;

For TDM: $\left(I_{\text{ph}},\ I_{\text{s1}},\ a_1,\ R_{\text{s}},\ R_{\text{sh}},\ I_{\text{s2}},\ a_2,\ I_{\text{s3}},\ a_3\right)$.

Objective Function: The GTO algorithm requires the objective function to effectively extract PV cell model parameters. The aim of the parameter extraction algorithm is to find model parameters that minimize the difference between the observed and computed current. The most correct set of parameter values will produce slightly larger or lower prediction values than the experimental ones. The objective function is a function that minimizes the difference between the experimental and predicted values. The root mean square error (RMSE) has been generally accepted as the objective function, and is given as [151]:

$$RMSE = \sqrt{\frac{1}{M}\sum_{j=1}^{M}\left(I_{\text{exp}}^{j} - I_{\text{calc}}^{j}\left(V_{\text{exp}}^{j}, x\right)\right)^2} \tag{23}$$

where the jth point experimental values for current and voltage are $I_{\exp}^{j}$ and $V_{\exp}^{j}$, respectively.

The accurate turbulent flow of water optimizer: The irregular fluctuation of turbulent water flow inspired Mojtaba Ghasemi et al. [147] to develop the turbulent flow of water-based optimization algorithm (TFWOA). In the water turbulent flow, the magnitude and speed direction are constantly changing in a circular form as the water flows down in a spiral manner. In the TFWOA algorithm, the whirlpool stands for natural random behavior that occurs in water bodies (seas, lakes, or rivers). The whirlpool's center acts as a sucking hole, which pulls every particle across it towards the center. In this algorithm, the initial population, consisting of N_{p} members, is divided equally to form N_{wh} groups which stand for the whirlpool sets. Then, the strongest member (having better objective function values, $f(X)$ of each set) is considered to be the whirlpool (Wh), which pulls the objects.

Every Wh acts as a pulling force which tries to unify the locations of all the elements inside its set (X) with its central position, by applying a centripetal force onto them and pulling them into the well. Here, the jth whirlpool pulls the ith object position to itself so that $X_i = Wh_j$. Notwithstanding, other whirlpools give some deviations (ΔX_i) because of the distance, $Wh - Wh_j$ separating them, as well as $f(X)$. Hence, the new position of the ith object is now $X_i^{\mathrm{new}} = Wh_j - \Delta X_i \ldots$, and the object, X, travels with the spiral angle δ across their whirlpool center as it moves towards it. Thus, the angle in each iteration is changing as in [115]:

$$\delta_i^{\mathrm{new}} = \delta_{\mathrm{i}} + r_1 * r_2 * \pi. \tag{24}$$

To continue with the model, one needs to compute the farthest and the nearest whirlpool, ΔX_i. Equation (25) shows the whirlpool with the smallest weighed distance from all objects, while Equation (26) is used to compute ΔX_i. The updated position of the particle is given by Equation (27) [115].

$$\Delta_t = f(Wh_t) * |Wh_t - \mathrm{sum}(X_i)|_{0.5}. \tag{25}$$

$$\begin{aligned} \Delta X_t \quad &= \left(\cos\left(\delta_i^{\mathrm{new}}\right) * r(1, D) * \left(Wh_f - X_i\right)\right. \\ &\quad - \sin\left(\delta_i^{\mathrm{new}}\right) * r(1, D) * (Wh_w - X_i) * \\ &\quad \left.\left(1 + \left|\cos\left(\delta_i^{\mathrm{new}}\right) - \sin\left(\delta_i^{\mathrm{new}}\right)\right|\right) \end{aligned} \tag{26}$$

$$X_i^{\mathrm{new}} = Wh_j - \Delta X_i. \tag{27}$$

where Wh_w shows the maximum and Wh_f the minimum whirlpools of Δ_t, while δ_i characterizes ith object's angle.

The centrifugal force, FE_i of the whirlpool, may sometimes be greater than the centripetal force, and may randomly move objects to a new location. Equation (27) models the random behavior of the centrifugal force in one dimension of the decision variables. To achieve this, FE_i is calculated according to the angle between the object and the whirlpool, as shown in Equation (27) [115]. Now, if the force is greater, a value is selected randomly in the range [0, 1], and the centrifugal action is carried out for a randomly chosen dimension, as demonstrated in Equation (28) [115].

$$FE_i = \left(\cos(\delta_i^{\mathrm{new}})^2 * \sin\left(\delta_i^{\mathrm{new}}\right)^2\right)^2 \tag{28}$$

$$X_{ip} = X_p^{\min} - r * \left(X_p^{\max} - X_p^{\min}\right) \tag{29}$$

Whirlpools interact with and displace one another. This behavior can be modeled in a similar way to the impact of the whirlpool on objects, where every whirlpool has the propensity to pull other whirlpools with centripetal force. The nearest whirlpool can mathematically be represented based on the minimum amount and its objective function, as shown in Equation (30). The position of the whirlpool is updated using Equations (31) and (32) [115].

$$\Delta_t = f(Wh_t) * \left|Wh_t - \mathrm{sum}\left(W_j\right)\right|^{0.5}. \tag{30}$$

$$Wh_j = r(1, D) * \left| \left(\cos\left(\delta_j^{\text{new}}\right) + \sin\left(\delta_j^{\text{new}}\right) \right| * \left(Wh_f - Wh_j \right) \tag{31}$$

$$\Delta Wh_j^{\text{new}} = Wh_f - Wh_j. \tag{32}$$

where δ_j is the hole angle value of the ith whirlpool.

When, finally, the strongest member has more strength than the new members of the whirlpool set, implying that the value of its objective function is less than the current whirlpool, it is selected to become the next whirlpool for the next iteration. Figure 5 show the flowchart of the TWFOA.

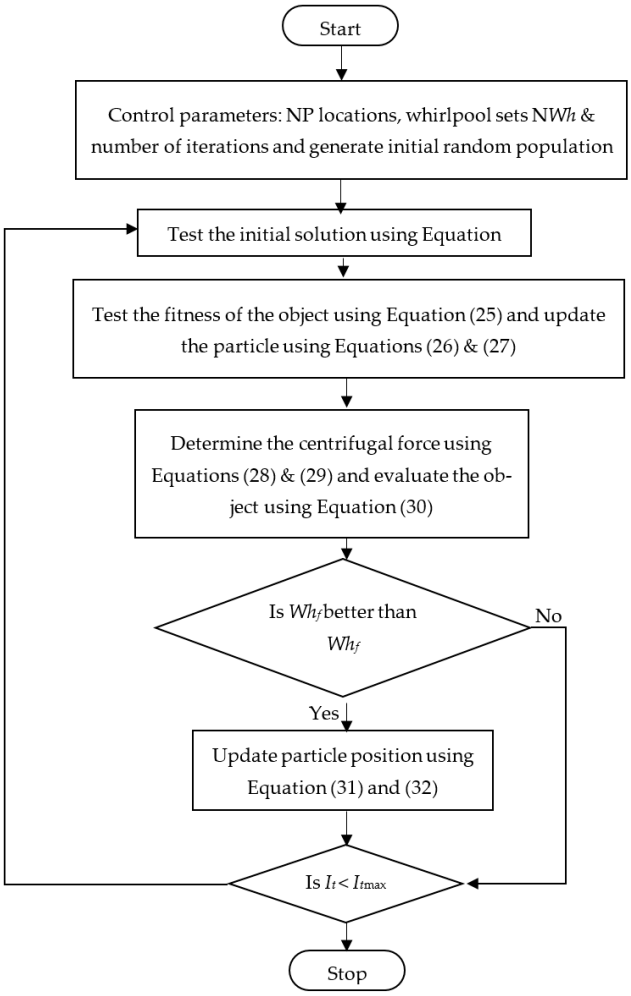

Figure 5. TFWOA algorithm flowchart [115].

Gorilla troops optimization (GTO): The GTO was inspired by the group behaviors of gorillas, where five strategies are identified. These strategies include migration to an undiscovered area, going to other gorillas, migrating in the direction of a location that has been identified, following the silva back, and competing for adult female gorillas. These strategies are mimicked and used to explain the exploration and exploitation of the optimization algorithm. The optimization process is divided into two phases: exploration and exploitation. Three strategies are employed during the exploration phase: migration to an undiscovered area, moving to other gorillas, and migration to the identified location. The remaining two strategies, following the silverback and competing for adult females, are used during the exploitation phase.

Exploration Phase: All gorillas have equal chances of being the candidate solution in GTO, and at each optimization step, the best candidate solution is chosen as the silverback gorilla. Three strategies are employed in this phase. They include migrations to an unidentified place to raise the exploration of GTO, movement to other gorillas have an

increased balance between exploration and exploitation, and migration in the direction of a location that has been identified to raise the GTO capability in searching for diverse optimization spaces. If the *rand* < parameter (p), migrating to an unidentified place strategy is chosen. When $rand \geq 0.5$, a movement to other gorillas' strategy is chosen, and migration in the direction of an identified location becomes the chosen strategy if $rand < 0.5$. These three strategies can be summarized mathematically as [152]:

$$GX(t+1) = \begin{cases} (\mathrm{UL} - \mathrm{LL}) \times r_1 + LL, \ rand < p, \\ (r_1 - C) \times X_r(t) + L \times H, rand \ \geq 0.5, \\ X(i) - L \times (L \times (X(t) - GX_r(t)) + r_3 \times (X(t) - (X(t) - GX_r(t))), rand < 0.5 \end{cases} \quad (33)$$

where $X(t)$ and $GX(t+1)$ are, respectively, the current vector of gorilla position and the candidate position vector of the gorilla in the next iteration t; *rand*, r_1, r_2, and r_3 represent random numbers in the range [0, 1]. The parameter p is the probability of choosing a migration strategy to an unidentified location, which must be specified in the range [0, 1], before starting the optimization operation. The X_r and GX_r parameters represent one designated member of the gorilla's population and one of the vectors of gorilla positions which can be a designated candidate, respectively. The lower and upper limits of the variables are LL and UL, respectively. The C, L, and H variables are calculated using Equations (35)–(37), respectively [152].

$$F = \cos(2 \times r_4) + 1 \quad (34)$$

$$C = F \times \left(1 - \frac{It}{MaxIt}\right), \quad (35)$$

$$L = C \times l, \quad (36)$$

$$H = Z \times X(t), \quad (37)$$

$$Z = [-C, C], \quad (38)$$

where the current iteration and total iteration optimization operation values are represented by It and $maxIt$, respectively. r_4 represents random values in the range 0 to 1. l and Z variables are random values in the range $[-1, 1]$ and $[-C, C]$, respectively.

The cost of the solution GX is assessed upon completion of the exploration phase. If the cost of $GX(t) < X(t)$, the GX solution will replace $X(t)$ solution and become the silverback—the best solution.

Exploitation Phase: The exploitation phase employs two strategies. One is "*following the silverback*" strategy and the other is "*competition for adult females*" strategy. A comparison of the value of C (computed using Equation (35)) with the W parameter will be shown shortly, and which strategy to choose is left for the leader of the gorilla group to make.

The leader of the group, who makes the decisions and guides others in the direction of food sources, is the silverback gorilla. This exploitation phase strategy is chosen if $C \geq W$. This is expressed mathematically as [152]:

$$GX(t+1) = L \times M \times (X(t) - X_{\text{silverback}}) + \mathrm{X(t)}, \quad (39)$$

where $X(t)$ and $X_{\text{silverback}}$ are the gorilla position vector and silverback gorilla position vector, respectively. $X_{\text{silverback}}$ offers the best solution. M is computed using [152]:

$$M = \left(\left| \frac{1}{N} \sum_{i=1}^{N} GX_i(t) \right|^g \right)^{\frac{1}{g}} \quad (40)$$

In iteration t, $GX(t)$ shows the position of each candidate gorilla's vector, and N represents the number of gorillas.

$$g = 2^L. \quad (41)$$

where L is computed with Equation (36).

The strategy of competition for adult females is chosen for exploitation if $C < W$. When young male gorillas mature, they compete violently with each other over selecting adult females. This is expressed mathematically as [152]:

$$GX(i) = X_{\text{silverback}} - (X_{\text{silverback}} \times Q - X(t) \times Q) + \text{A}, \tag{42}$$

$$Q = 2 \times r_5 - 1, \tag{43}$$

$$A = \beta \times E, \tag{44}$$

$$E = \begin{cases} N_1 rand \geq 0.5 \\ N_2 rand < 0.5' \end{cases} \tag{45}$$

where Q is impact force, and r_5 is random values in the range [0, 1]. A represents the degree of violence when there are conflicts, β is set before optimization, and E is used to simulate the violence effect on the solutions' dimensions.

At the end of the exploitation phase, the cost of all GX solutions are checked, and if the cost of $GX(t) < X(t)$, then $GX(t)$ will replace $X(t)$ solution and become the best solution (the silverback). The flow chart that demonstrates how GTO is used for solar cell models' parameter extraction is illustrated in Figure 6.

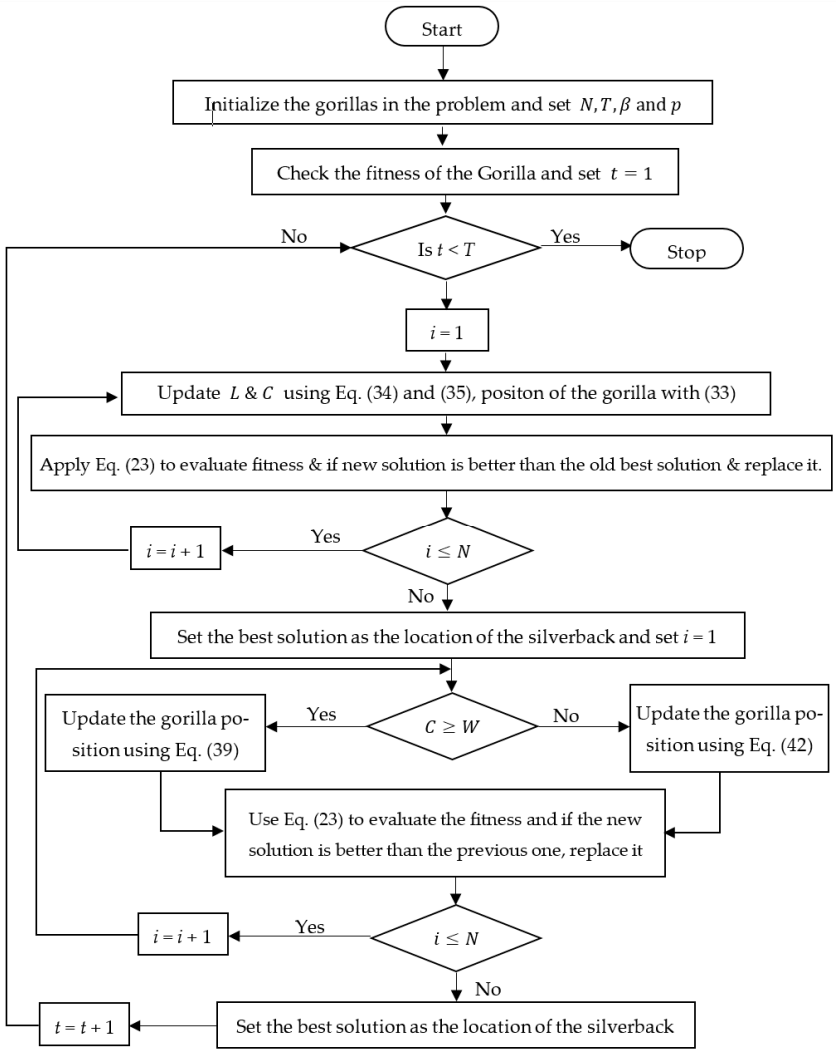

Figure 6. GTO algorithm flowchart [152].

4. Performance Evaluation

4.1. Matrices for Model Performance Evaluation

Solar PV electricity-generating systems are now becoming a significant part of the main electricity grid. The main grid needs to plan, manage, and distribute the generated electrical energy. The main grid needs the individual constituent sources of electric energy generation to meet their electrical energy commitment to the center. Hence, it is essential to evaluate the accuracy of the predicting model. Having a standard way to evaluate the performance of forecasting models would help to standardize the comparison of different models' performances. Among some of the many tools which have been used to analyze the PV output power generation prediction accuracy [10] are MSE [10], RMSE [153], nRMSE [154], MAE [23], MAPE [155], MRE [156], and MBE [59]. They are expressed mathematically as:

$$\text{MSE} = \frac{1}{N}\sum_{i=1}^{N}(W_{\text{forecasted}} - W_{\text{measured}})^2 \tag{46}$$

$$\text{RMSE} = \sqrt{\frac{1}{N}\sum_{i=1}^{N}(W_{\text{forecasted}} - W_{\text{measured}})^2} \tag{47}$$

$$\text{nRMSE} = \left(\sqrt{\frac{1}{N}\sum_{i=1}^{N}(W_{\text{forecasted}} - W_{\text{measured}})^2}\right) \times \frac{100}{W_{\text{measured(max)}}} \tag{48}$$

$$\text{MAE} = \frac{1}{N}\sum_{i=1}^{N}|W_{\text{forecasted}} - W_{\text{measured}}| \tag{49}$$

$$\text{MAPE} = \frac{1}{N}\sum_{i=1}^{N}\frac{|W_{\text{forecasted}} - W_{\text{measured}}|}{W_{\text{measured}}} \times 100\% \tag{50}$$

$$\text{MRE} = \frac{1}{N}\sum_{i=1}^{N}\frac{W_{\text{forecasted}} - W_{\text{measured}}}{W_{\text{total}}} \times 100\% \tag{51}$$

$$\text{MBE} = \frac{1}{N}\sum_{i=1}^{N}(W_{\text{forecasted}} - W_{\text{measured}}) \tag{52}$$

where $W_{\text{forecasted}}$, W_{measured}, $W_{\text{measured(max)}}$, and W_{total} are, respectively, the predicted, measured, maximum measured (at this scale), and the installation capacity of the PV output power at a particular instant in time.

4.2. Evaluating the Performance of Some Selected Forecasting Models

The persistence or the primary model has been used extensively as a benchmark to evaluate the performance of simple and complex power generation modeling techniques. This technique shows reasonable accuracy when the forecast horizon is within the neighborhood of a few hours or days. However, its accuracy begins to reduce as the number of hours increases. It has been successfully used to forecast PV output power for similar sunny days nearby. However, its accuracy decreases with increasing cloud coverage, as well as when the period of the forecast horizon is more than 1 h [25]. This method is not sufficient to be used as a PV output forecasting technique, but serves as a benchmark for evaluating the performance of the other methods [108].

One instance of a linear technique that uses statistical methods to correlate historical input data is ARMA. This technique handles different types of time-series data to extract statistical properties from them, but the data need to be stationary. An improved version of ARMA, which can [109,110] process nonstationary time-series data, is ARIMA [157], which can also handle sharp changes in irradiance [25] with higher accuracy. The ability to handle sharp changes in the meteorological parameter is a great advantage, especially in cases where sharp change exists in the weather data. The ARIMA is more computationally

intensive when compared to ARMA because it incorporates integration and summation functions in its procedure, which is one weakness of this technique.

The ANN technique came into existence to take care of the linear methods' inability to handle the nonlinear relationship in the historical time-series data. Its popularity comes from its unprecedented ability to extract features from the data during the training phase to produce results with greater accuracy. This method is robust and self-adaptive; it also has fault tolerance and strong inference-drawing capabilities. Models developed with ANN outperform their linear counterparts where adaptability is concerned [109,110]. One of the weaknesses of the ANN method is that it is more complex, as it uses multi-layered architecture. Another is that it requires an initially random set of data, which may affect the accuracy of its results.

Fuzzy logic provides a powerful and advantageous way of modeling parameters, based on the inference rule. It has been applied in medium-term forecasting horizons because it can capture uncertainties in historical data [158]. Again, its rules are based on linguistics, making it easy to apply the statistical method to decision-making [159,160]. The ANFIS method has also been developed, which combines fuzzy logic and NNs [161]. ANFIS had a 95% improvement in accuracy from the traditional fuzzy logic technique. The fuzzy logic method has a longer execution time requirement than SVM, which limits performance and is the drawback of this method [162].

SVM is a robust and very flexible nonlinear modeling technique which has been applied extensively in wind energy output power forecasting, and has recently moved to forecast PV output power. SVM's outstanding advantage is its ability to learn without heavy dependence on prior knowledge, unlike ANN [163]. It also does not have local minima problems, as the NNs do [164]. It allows complex mathematical problems that are associated with predicting PV output power to be simplified [165]. The performance of SVM is susceptible to the choice of the penalty factor (C), the tube radius (ϵ), and the kernel function parameters used in designing the forecasting model. Making the right choices for these parameters is a difficult task.

The main aim of designing a forecasting model is to make accurate predictions. Short-term forecast horizon models used to predict PV output power should have RMSE forecast errors of less than 20% [166]. The application of the hybrid model technique to forecast PV output power generation has dominated the technology space due to its prediction accuracy. Table 2 presents a tabular review of recent works on PV output power forecasting, showing the technique employed and its performance (in terms of error analysis). Section 6 presents the different error analysis methods listed in Table 2.

Table 2. A summary of the literature review of PV output power forecasting, showing references, forecast horizon, technique, and results.

Ref.	Forecast Horizon	Forecast Method	Forecast Error
[167]	Short-term	RNN KNN GA	RMSE = 56.89%, MAE = 20.18%, rRME = 7.54%, rMAE = 4.49% RMSE = 57.48%, MAE = 20.94%, rRME = 7.58%, rMAE = 4.58% RMSE = 35.50%, MAE = 26.74%, rRME = 5.95%, rMAE = 5.17%
[168]	Very short-term	Persistence, MPL, CNN, LSTM	RMSE = 15.3%
[169]	Short-term	Similarity algorithm, KNN, NARX, and smart persistence models	RMSE = 2.3%
[121]	Short-term	Physics-constrained long-term memory (PC-LSTM) network	MAE = 3.13%
[170]	Short-term	Adaptive-network-based fuzzy inference system (ANFIS) and PSO-ANN models.	RMSE = 0.1184%
[171]	Short-term	Vector AR exogenous	NRMSE = 8.5%
[73]	Short-term	Physical model	Normalized MAE (NMAE) < 1% & weighted MAE < 2%
[155]	Short-term	Back-propagation based ANN model	MAPE = 7.65%

Table 2. *Cont.*

Ref.	Forecast Horizon	Forecast Method	Forecast Error
[172]	Short-term	Elman NN	Mean absolute percentage error (MAPE) = 16.83%
[173]	Short-term	GA+ PSO + ANFIS	NRMSE = 5.48%
[8]	Short-term	RF, fuzzy C-means (FCM), sparse Gaussian process (SPGP), and improved grey wolf optimizer	RMSE = 6.5%
[174]	Short-term	Hybrid model of wavelet decomposition and ANN	RMSE value between 7.193% and 19.663%
[156]	Short-term	Non–parametric model	cv-Mean bias error < 1.3%
[175]	Short-term	K-means clustering method	MAPE ≈ 11%
[176]	Short-term	Statistical methods based on multiple regression analysis and Elman ANN	NMAE values between 6.50% and 19.49% and nRMSE values between 10.91% and 23.99%
[177]	Short-term	SOM and RBFNN	MAPE values between 8.29% and 10.80%
[178]	Short-term	WT, fuzzy ARTMAP, and firefly	MAPE 3.38−11.83% and nRMSE 12.11−13.13%
[179]	Short-term	GA-based NN	Error 8.00%
[88]	Short-term	ANN and similar day selection algorithm	MAPE of 10.06% (on sunny day) and 18.89% (on rainy day)
[180]	Short-term	Stepwise regression, GRNN, FFNN, and MLR	RMSE = 2.74%
[83]	Short-term	WT and RBFNN	MAPE 2.38% (on sunny day) and 4.08% (on cloudy day)
[174]	Short-term	Hybrid model of wavelet decomposition and ANN	RMSE values between 7.193−19.663%

5. Model Optimization

Designing a reliable off (or on) -grid PV power generation system requires the ability to accurately predict its power output for planning, management, and distribution. Hence, the goal is to ensure high accuracy of the forecasting model. Forecast model performance depends on the model's parameters. The forecast horizon, several hidden units, and neurons are the selection parameters of ANN, while the penalty factor, tube radius, and kernel function parameter are the hyperparameters of the SVR. The forecasting model's performance depends on the value of these parameters, so care should be taken when choosing values for them. When designing a forecast model, researchers guess values for these parameters from their experience and modify them in order to obtain the desired accuracy.

Almeida et al. [156] stated that choosing the correct number of neurons is essential when designing a neural network for PV output power forecasting. He obtained the correct number of hidden units by guessing, and then improving his guess during the next trial to minimize forecasting error. Reikard [109] developed a feedforward ANN with the backpropagation method. They also obtained the appropriate number of hidden units and neurons by the trial-and-error method. Liu et al. [155] used the ANN technique to design a model which predicts the PV power for a forecast horizon of 24 h. Nagi et al. [181] obtained their desired accuracy by starting with a guess and improving upon it in each iteration. Xu et al. [182] designed a weighted SVM for short-term event horizon prediction of PV output power generation. They also chose values for ϵ and C parameters by the trial-and-error method. A technique to forecast PV output power generation using a combination of weather classification and SVM was suggested by [55]. They obtain the optimal values for hyper-parameters by the trial-and-error method [36]. Using a good optimization technique is important when choosing network parameters, as the model's performance depends on it.

Many tools have been used to choose optimal values for NN hyperparameters, of which GA is often used. It works by following the way that chromosomes duplicate new DNA strings by bringing together elements from two other chromosome strands, referred to as crossover [183]. This technique was used to optimize the weights and thresholds of

BPNN, which improved the accuracy of the model [179]. Pedro and Coimbra [23] agreed that using the GA to optimize the model parameters would improve the performance prediction model. It should be noted that other optimization tools have been developed over the years, such as the fruit fly optimization algorithm (FOA), particle swarm optimization (PSO) [184], firefly (FF) [178], chaotic artificial bee colony algorithm [185], grid search [186], chaotic ant swarm optimization (CAS) [187], immune algorithm (IA) [100], and ant colony optimization (ACO) [188]. Application of these algorithms in and of themselves does not guarantee high accuracy. The prediction accuracy also depends on the correct definition of the input parameters and algorithmic process for extracting valid output power.

6. Challenges of Photovoltaic Power Forecasting

Solar PV output power forecasting has its challenges and limitations, as is the case with any other predictive analytics. One of the main limitations encountered is the accurate prediction of future weather conditions when applying physical and indirect methods that require future weather parameters as input [189]. Another limitation is the issue of having a huge amount of data to be processed when applying statistical methods. Although a large amount of data allows this technique to make better predictions, the processing the data consumes significant machine resources, which is also a weakness of this method. In addition, once a large amount of data is being processed, there is often a compromise on the output's speed and accuracy, particularly for generation plants where real-time data output is required.

In most statistical and hybrid approaches, it is usually considered that a complex model will obtain more accurate results. This is not always a guaranteed scenario, as a simpler technique may sometimes yield higher accuracy if the input parameters are properly filtered and pre-processed. This poses a challenge, similar to the view expressed by the authors in [12], in selecting the right model and input parameters.

Furthermore, there is the challenge of cell/module degradation and site-specific losses, which negatively impact medium- and long-term power forecasting estimates. Since forecasting models are based on input weather conditions, historical data, or both, the forecasted data may deviate significantly when unexpected adverse weather conditions occur. The occurrence may accelerate the degradation of the installed solar cells/modules in a manner different from the predefined constant degradation factor that has been applied in the forecasting model. Thus, even when site-specific modeling has been conducted, there may be a need to constantly review the model's input parameters over time based on the degradation of the solar PV modules.

7. Conclusions

This work has systematically reviewed the current trends in PV output power generation forecasting technologies. Every model has its merits and demerits, depending on the case study under investigation. Developing a model for PV output power generation prediction has drawn much attention to the energy industry for adequate utility-scale energy planning. Much research has been conducted to develop accurate PV output power forecasting models, and has yielded highly predictive models. However, some areas require improvement, such as developing a high accuracy forecasting model with less weight attached to weather prediction accuracy. Another is designing an optimal PV output power forecasting model with a reduced computational requirement, which can simultaneously provide a high level of accuracy for medium- to long-term forecasting.

Recently, machine learning and artificial intelligence (AI) processes have been applied towards solar PV output power forecasting technologies, because of their relatively high accuracy and capability to learn from continuously updated historical data. It is envisaged that further advancement in AI and big data will aid in breaking new ground in predicting solar PV output power.

Funding: This research was made possible through financial support in part by Govan Mbeki Research and Development Centre. We also thank the Department of Science and Innovation, Eskom, and the National Research Foundation of South Africa for financially supporting this research.

Institutional Review Board Statement: Not applicable.

Informed Consent Statement: Not applicable.

Data Availability Statement: Not applicable.

Acknowledgments: We acknowledge the support of the academic staff of FHIT and my wife Chidinma Iheanetu who was on my side all the way till the successful completed of this work.

Conflicts of Interest: The authors declare no conflict of interest.

References

1. IEA. 2022 Solar PV Report. Available online: https://www.iea.org/reports/solar-pv (accessed on 13 August 2022).
2. Woyte, A.; Thong, V.; Belmans, R.; Nijs, J. Voltage fluctuations on distribution level introduced by photovoltaic systems. *IEEE Trans. Energy Convers.* **2006**, *21*, 202–209. [CrossRef]
3. Strzalka, A.; Alam, N.; Duminil, E.; Coors, V.; Eicker, U. Large scale integration of photovoltaics in cities. *Appl. Energy* **2012**, *93*, 413–421. [CrossRef]
4. Das, U.; Tey, K.; Idna Idris, M.; Mekhilef, S. Maximum Power Flow Management for Stand-alone PV Based Battery Charging System. In Proceedings of the 10th International Conference Power Electron, Busan, Republic of Korea, 27–30 May 2019. [CrossRef]
5. Feilat, E.; Azzam, S.; Al-Salaymeh, A. Impact of large PV and wind power plants on voltage and frequency stability of Jordan's national grid. *Sustain. Cities Soc.* **2018**, *36*, 257–271. [CrossRef]
6. Gensler, A.; Henze, J.; Sick, B.; Raabe, N. Deep Learning for solar power forecasting—An approach using AutoEncoder and LSTM Neural Networks. In Proceedings of the IEEE International Conference on Systems, Man, and Cybernetics (SMC), Budapest, Hungary, 9–12 October 2016. [CrossRef]
7. Tuohy, A.; Zack, J.; Haupt, S.; Sharp, J.; Ahlstrom, M.; Dise, S.; Grimit, E.; Mohrlen, C.; Lange, M.; Casado, M.; et al. Solar Forecasting: Methods, Challenges, and Performance. *IEEE Power Energy Mag.* **2015**, *13*, 50–59. [CrossRef]
8. El Hendouzi, A.; Bourouhou, A. Solar Photovoltaic Power Forecasting. *J. Electr. Comput. Eng.* **2020**, *2020*, 8819925. [CrossRef]
9. Das, K.; Tey, K.; Seyedmahmoudian, M.; Mekhilef, S.; Idris, M.; Deventer, W.; Horan, B.; Stojcevski, A. Forecasting of photovoltaic power generation and model optimization: A review. *Renew. Sustain. Energy Rev.* **2018**, *81*, 912–928. [CrossRef]
10. Mellit, A.; Pavan, A.; Ogliari, E.; Leva, S.; Lughi, V. Advanced Methods for Photovoltaic Output Power Forecasting: A Review. *Appl. Sci.* **2020**, *10*, 487. [CrossRef]
11. Li, P.; Zhou, K.; Yang, S. Photovoltaic Power Forecasting: Models and Methods. In Proceedings of the 2nd IEEE Conference Energy Internet Energy System Integration, Beijing, China, 20–22 October 2018. [CrossRef]
12. Dolara, A.; Grimaccia, F.; Leva, S.; Mussetta, M.; Ogliari, E. A Physical Hybrid Artificial Neural Network for Short Term Forecasting of PV Plant Power Output. *Energies* **2015**, *8*, 1138–1153. [CrossRef]
13. Monteiro, C.; Alfredo Fernandez-Jimenez, L.; Ramirez-Rosado, I.; Muñoz-Jimenez, A.; Lara-Santillan, P. Short-Term Forecasting Models for Photovoltaic Plants: Analytical versus Soft-Computing Techniques. *Math. Probl. Eng.* **2013**, *2013*, 767284. [CrossRef]
14. Massidda, L.; Marrocu, M. Use of Multilinear Adaptive Regression Splines and numerical weather prediction to forecast the power output of a PV plant in Borkum, Germany. *Sol. Energy* **2017**, *146*, 141–149. [CrossRef]
15. Soman, S.; Zareipour, H.; Malik, O.; Mandal, P. A review of wind power and wind speed forecasting methods with different time horizons. In Proceedings of the North American Power Symposium, Arlington, TX, USA, 26–28 September 2010. [CrossRef]
16. Zhang, J.; Florita, A.; Hodge, B.; Lu, S.; Hamann, H.; Banunarayanan, V.; Brockway, A. A suite of metrics for assessing the performance of solar power forecasting. *Sol. Energy* **2015**, *111*, 157–175. [CrossRef]
17. Blanc, P.; Remund, J.; Vallance, L. Short-term solar power forecasting based on satellite images. In *Renewable Energy Forecasting from Model to Applications*; Woodhead Publishing: Cambridge, UK, 2017; pp. 179–198. [CrossRef]
18. Gueymard, C. Clear-sky irradiance predictions for solar resource mapping and large-scale applications: Improved validation methodology and detailed performance analysis of 18 broadband radiative models. *Sol. Energy* **2012**, *86*, 2145–2169. [CrossRef]
19. Sengupta, M.; Habte, A.; Wilbert, S.; Gueymard, C.; Remund, J. *Best Practices Handbook for the Collection and Use of Solar Resource Data for Solar Energy Applications*, 3rd ed.; National Renewable Energy Laboratory: Golden, CO, USA, 2021. [CrossRef]
20. Boilley, A.; Thomas, C.; Marchand, M.; Wey, E.; Blanc, P. The Solar Forecast Similarity Method: A New Method to Compute Solar Radiation Forecasts for the Next Day. *Energy Procedia* **2016**, *91*, 1018–1023. [CrossRef]
21. Dambreville, R.; Blanc, P.; Chanussot, J.; Boldo, D. Very short term forecasting of the Global Horizontal Irradiance using a spatio-temporal autoregressive model. *Renew. Energy* **2014**, *72*, 291–300. [CrossRef]
22. Voyant, C.; Haurant, P.; Muselli, M.; Paoli, C.; Nivet, M.L. Time series modeling and large scale global solar radiation forecasting from geostationary satellites data. *Sol. Energy* **2014**, *102*, 131–142. [CrossRef]

23. Pedro, H.; Coimbra, C. Assessment of forecasting techniques for solar power production with no exogenous inputs. *Sol. Energy* **2012**, *86*, 2017–2028. [CrossRef]
24. Kleissi, J. Current State of the Art in Solar Power Forecasting. California Renewable Energy Forecasting, Resource Data and Mapping. 2010. Available online: https://escholarship.org/uc/item/4fx8983f (accessed on 13 October 2022).
25. Diagne, M.; David, M.; Lauret, P.; Boland, J.; Schmutz, N. Review of solar irradiance forecasting methods and a proposition for small-scale insular grids. *Renew. Sustain. Energy Rev.* **2013**, *27*, 65–76. [CrossRef]
26. Coimbra, F.; Kleissl, J.; Marquez, R. Overview of solar-forecasting methods and a metric for accuracy evaluation. In *Solar Energy Forecasting and Resource Assessment*, 1st ed.; Kleissl, J., Ed.; Academic Press: Cambridge, MA, USA, 2013; pp. 171–194.
27. Lorenz, E.; Hammer, A.; Heinemann, D. Short term forecasting of solar radiation based on satellite data. In Proceedings of the ISES Europe Solar Congress, Freiburg, Germany, 20 June 2004.
28. Wang, G.; Su, Y.; Shu, L. One-day-ahead daily power forecasting of photovoltaic systems based on partial functional linear regression models. *Renew. Energy* **2016**, *96*, 469–478. [CrossRef]
29. Wang, H.; Yi, H.; Peng, J.; Wang, G.; Liu, Y.; Jiang, H.; Liu, W. Deterministic and probabilistic forecasting of photovoltaic power based on deep convolutional neural network. *Energy Convers. Manag.* **2017**, *153*, 409–422. [CrossRef]
30. Cervone, G.; Clemente-Harding, L.; Alessandrini, S.; Delle Monache, L. Short-term photovoltaic power forecasting using Artificial Neural Networks and an Analog Ensemble. *Renew. Energy* **2017**, *108*, 274–286. [CrossRef]
31. Kudo, M.; Takeuchi, A.; Nozaki, Y.; Endo, H.; Sumita, J. Forecasting Electric Power Generation in a Photovoltaic Power System for an Energy Network. *Electr. Energy Jpn.* **2009**, *167*, 16–23. [CrossRef]
32. Zhen, Z.; Fei, W.; Sun, Y.; Zengqiang, M.; Liu, C.; Wang, B.; Jing, L. SVM based cloud classification model using total sky images for PV power forecasting. In Proceedings of the IEEE Power Energy Society Innovative Smart Grid Technologies Conference, Washington, DC, USA, 18–20 February 2015. [CrossRef]
33. Abdel-Nasser, M.; Mahmoud, K. Accurate photovoltaic power forecasting models using deep LSTM-RNN. *Neural Comput. Appl.* **2019**, *31*, 2727–2740. [CrossRef]
34. Qing, X.; Niu, Y. Hourly day-ahead solar irradiance prediction using weather forecasts by LSTM. *Energy* **2018**, *148*, 461–468. [CrossRef]
35. Thevenard, D.; Pelland, S. Estimating the uncertainty in long-term photovoltaic yield predictions. *Sol. Energy* **2013**, *91*, 432–445. [CrossRef]
36. Yang, H.T.; Huang, C.M.; Huang, Y.C.; Pai, Y.S. A weather-based hybrid method for 1-day ahead hourly forecasting of PV power output. *IEEE Trans. Sustain. Energy* **2014**, *5*, 917–926. [CrossRef]
37. Yang, X.; Ren, J.; Yue, H. Photovoltaic power forecasting with a rough set combination method. In Proceedings of the 11th UKACC International Conference Control, Belfast, UK, 31 August–2 September 2016. [CrossRef]
38. Tanaka, K.; Uchida, K.; Ogimi, K.; Goya, T.; Yona, A.; Senjyu, T.; Funabashi, T.; Kim, C.H. Optimal operation by controllable loads based on smart grid topology considering insolation forecasted error. *IEEE Trans. Smart Grid.* **2011**, *2*, 438–444. [CrossRef]
39. Senjyu, T.; Toshiaki, K.; Atsushi, Y.; Naomitsu, U.; Toshihisa, F.; Fujihiro, Y.; Shigeyuki, S. Output power control for large wind power penetration in small power system. In Proceedings of the IEEE Power Engineering Society General Meeting, Tampa, FL, USA, 24–28 June 2007. [CrossRef]
40. Zhang, P.; Takano, H.; Murata, J. Daily solar radiation prediction based on wavelet analysis. In Proceedings of the SICE Annual Conference, Tokyo, Japan, 13–18 September 2011.
41. Capizzi, G.; Napoli, C.; Bonanno, F. Innovative second-generation wavelets construction with recurrent neural networks for solar radiation forecasting. *IEEE Trans. Neural Netw. Learn. Syst.* **2012**, *23*, 1805–1815. [CrossRef]
42. Cao, S.; Weng, W.; Chen, J.; Liu, W.; Yu, G.; Cao, J. Forecast of solar irradiance using chaos optimization neural networks. In Proceedings of the Asia-Pacific Power Energy Engineering Conference, Wuhan, China, 27–31 March 2009. [CrossRef]
43. Wang, F.; Mi, Z.; Su, S.; Zhao, H. Short-Term Solar Irradiance Forecasting Model Based on Artificial Neural Network Using Statistical Feature Parameters. *Energies* **2012**, *5*, 1355–1370. [CrossRef]
44. Hocaoğlu, F.O.; Gerek, Ö.N.; Kurban, M. Hourly solar radiation forecasting using optimal coefficient 2-D linear filters and feed-forward neural networks. *Sol. Energy* **2008**, *82*, 714–726. [CrossRef]
45. Patarau, T.; Petreus, D.; Etz, R. Analysis and optimization of a geothermal, biomass, solar hybrid system: An application of PV Sol software. In Proceedings of the 38th International Spring Seminar on Electronics Technology (ISSE), Eger, Hungary, 6–10 May 2015. [CrossRef]
46. Kandasamy, C.; Prabu, P.; Niruba, K. Solar potential assessment using PVSYST software. In Proceedings of the International Conference on Green Computing, Communication and Conservation of Energy (ICGCE), Chennai, India, 12–14 December 2013. [CrossRef]
47. Umer, F.; Aslam, M.; Rabbani, M.; Hanif, M.; Naeem, N.; Abbas, M. Design and Optimization of Solar Carport Canopies for Maximum Power Generation and Efficiency at Bahawalpur. *Int. J. Photoenergy* **2019**, *2019*, 6372503. [CrossRef]
48. Gandoman, F.; Raeisi, F.; Ahmadi, A. A literature review on estimating of PV-array hourly power under cloudy weather conditions. *Renew. Sustain. Energy Rev.* **2016**, *63*, 579–592. [CrossRef]
49. Da Silva Fonseca, J.; Oozeki, T.; Ohtake, H.; Takashima, T.; Ogimoto, K. Regional forecasts of photovoltaic power generation according to different data availability scenarios: A study of four methods. *Prog. Photovolt. Res. Appl.* **2015**, *23*, 1203–1218. [CrossRef]

50. Saint-Drenan, Y.; Good, G.; Braun, M.; Freisinger, T. Analysis of the uncertainty in the estimates of regional PV power generation evaluated with the upscaling method. *Sol. Energy* **2016**, *135*, 536–550. [CrossRef]
51. Huang, Y.; Lu, J.; Liu, C.; Xu, X.; Wang, W.; Zhou, X. Comparative study of power forecasting methods for PV stations. In Proceedings of the 2010 International Conference on Power System Technology (POWERCON2010), Zhejiang, China, 24–28 October 2010. [CrossRef]
52. Bracale, A.; Caramia, P.; Carpinelli, G.; Rita, A.; Fazio, D.; Ferruzzi, G. A Bayesian Method for Short-Term Probabilistic Forecasting of Photovoltaic Generation in Smart Grid Operation and Control. *Energies* **2013**, *6*, 733–747. [CrossRef]
53. Alessandrini, S.; Delle Monache, L.; Sperati, S.; Cervone, G. An analog ensemble for short-term probabilistic solar power forecast. *Appl. Energy* **2015**, *157*, 95–110. [CrossRef]
54. Alfadda, A.; Adhikari, R.; Kuzlu, M.; Rahman, S. Hour-ahead solar PV power forecasting using SVR based approach. In Proceedings of the IEEE Power & Energy Society Innovative Smart Grid Technologies Conference (ISGT), Washington, DC, USA, 23–26 April 2017. [CrossRef]
55. Alhakeem, D.; Mandal, P.; Haque, A.; Yona, A.; Senjyu, T.; Tseng, T. A new strategy to quantify uncertainties of wavelet-GRNN-PSO based solar PV power forecasts using bootstrap confidence intervals. In Proceedings of the 2015 IEEE Power & Energy Society General Meeting, Denver, CO, USA, 26–30 July 2015.
56. Catalão, J.; Pousinho, H.; Mendes, V. Hybrid wavelet-PSO-ANFIS approach for short-term electricity prices forecasting. *IEEE Trans. Power Syst.* **2011**, *26*, 137–144. [CrossRef]
57. Conejo, A.; Plazas, M.; Espínola, R.; Molina, A. Day-ahead electricity price forecasting using the wavelet transform and ARIMA models. *IEEE Trans. Power Syst.* **2005**, *20*, 1035–1042. [CrossRef]
58. Azadeh, A.; Ghaderi, S.F.; Sohrabkhani, S. Forecasting electrical consumption by integration of Neural Network, time series and ANOVA. *Appl. Math. Comput.* **2007**, *186*, 1753–1761. [CrossRef]
59. Raza, M.; Nadarajah, M.; Ekanayake, C. On recent advances in PV output power forecast. *Sol. Energy* **2016**, *136*, 124–144. [CrossRef]
60. Shi, J.; Lee, W.J.; Liu, Y.; Yang, Y.; Wang, P. Forecasting power output of photovoltaic systems based on weather classification and support vector machines. *IEEE Trans. Ind. Appl.* **2012**, *48*, 1064–1069. [CrossRef]
61. Perez, R.; Kivalov, S.; Schlemmer, J.; Hemker, K.; Renné, D.; Hoff, T. Validation of short and medium term operational solar radiation forecasts in the US. *Sol. Energy* **2010**, *84*, 2161–2172. [CrossRef]
62. Antonanzas, J.; Osorio, N.; Escobar, R.; Urraca, R.; Martinez-de-Pison, F.; Antonanzas-Torres, F. Review of photovoltaic power forecasting. *Sol. Energy* **2016**, *136*, 78–111. [CrossRef]
63. Huang, R.; Huang, T.; Gadh, R.; Li, N. Solar generation prediction using the ARMA model in a laboratory-level micro-grid. In Proceedings of the IEEE 3rd International Conference on Smart Grid Communications, Tainan, China, 5–8 November 2012. [CrossRef]
64. Rajagopalan, S.; Santoso, S. Wind power forecasting and error analysis using the autoregressive moving average modeling. In Proceedings of the 2009 IEEE Power & Energy Society General Meeting, Calgary, AB, Canada, 26–30 July 2009. [CrossRef]
65. Boland, J. Time series modelling of solar radiation. In *Modeling Solar Radiation at the Earth's Surface*; Badescu, V., Ed.; Springer: Berlin/Heidelberg, Germany, 2008; pp. 283–312. [CrossRef]
66. Box, G.; Jenkins, G.; Reinsel, G.; Ljung, G. *Time Series Analysis: Forecasting and Control*, 5th ed.; Wiley: Hoboken, NJ, USA, 2015.
67. Wan Ahmad, W.; Ahmad, S. Arima model and exponential smoothing method: A comparison. In Proceedings of the AIP Conference Proceedings, Sydney, Australia, 27–29 November 2013. [CrossRef]
68. Oudjana, S.; Hellal, A.; Mahamed, I. Short term photovoltaic power generation forecasting using neural network. In Proceedings of the 11th International Conference on Environment and Electrical Engineering (EEEIC), Venice, Italy, 18–25 May 2012. [CrossRef]
69. Ostertagova, E.; Ostertag, O. Forecasting using simple exponential smoothing method. *Acta Electrotech. Inform.* **2012**, *12*, 62–66. [CrossRef]
70. Holt, C. Forecasting seasonals and trends by exponentially weighted moving averages. *Int. J. Forecast.* **2004**, *20*, 5–10. [CrossRef]
71. Kalekar, P. Time series Forecasting using Holt-Winters Exponential Smoothing. *Kanwal Rekhi Sch. Inf. Technol.* **2004**, *4329008*, 1–13.
72. Winters, P. Forecasting Sales by Exponentially Weighted Moving Averages. *Manag. Sci.* **1960**, *6*, 324–342. [CrossRef]
73. Dolara, A.; Leva, S.; Manzolini, G. Comparison of different physical models for PV power output prediction. *Sol. Energy* **2015**, *119*, 83–99. [CrossRef]
74. Chu, Y.; Urquhart, B.; Gohari, S.; Pedro, H.; Kleissl, J.; Coimbra, C. Short-term reforecasting of power output from a 48 MWe solar PV plant. *Sol. Energy* **2015**, *112*, 68–77. [CrossRef]
75. Aminzadeh, F.; De Groot, P. *Neural Networks and Other Soft Computing Techniques with Applications in the Oil Industry*; Eage Publications: Lancaster, OH, USA, 2006.
76. Hossain, M.; Ong, Z.; Ismail, Z.; Noroozi, S.; Khoo, S. Artificial neural networks for vibration based inverse parametric identifications: A review. *Appl. Soft Comput.* **2017**, *52*, 203–219. [CrossRef]
77. Mellit, A.; Kalogirou, S. Artificial intelligence techniques for photovoltaic applications: A review. *Prog. Energy Combust. Sci.* **2008**, *34*, 574–632. [CrossRef]
78. Isa, I.; Omar, S.; Saad, Z.; Noor, N.; Osman, M. Weather forecasting using photovoltaic system and Neural Network. In Proceedings of the 2nd International Conference on Computational Intelligence, Communication Systems and Networks, Liverpool, UK, 28–30 July 2010. [CrossRef]

79. Zhang, Y.; Chen, G.; Malik, O.; Hope, G. An Artificial Neural Network Based Adaptive Power System Stabilizer. *IEEE Trans. Energy Convers.* **1993**, *8*, 71–77. [CrossRef]
80. Tasre, M.; Bedekar, P.; Ghate, V. Daily peak load forecasting using ANN. In Proceedings of the Nirma University International Conference on Engineering NUiCONE, Ahmedabad, India, 8–10 December 2011. [CrossRef]
81. Malki, H.; Karayiannis, N.; Balasubramanian, M. Short-term electric power load forecasting using feedforward neural networks. *Expert Syst.* **2004**, *21*, 157–167. [CrossRef]
82. Gupta, M.; Jin, L.; Homma, N. *Static and Dynamic Neural Networks: From Fundamentals to Advanced Theory*; John Wiley & Sons: Hoboken, NJ, USA, 2004.
83. Mandal, P.; Madhira, S.T.S.; Ul Haque, A.; Meng, J.; Pineda, R.L. Forecasting Power Output of Solar Photovoltaic System Using Wavelet Transform and Artificial Intelligence Techniques. *Procedia Comput. Sci.* **2012**, *12*, 332–337. [CrossRef]
84. Halden, U.; Cali, U.; Dynge, M.; Stekli, J.; Bai, L. DLT-based equity crowdfunding on the techno-economic feasibility of solar energy investments. *Sol. Energy* **2021**, *227*, 137–150. [CrossRef]
85. Li, H.; Guo, S.; Li, C.; Sun, J. A hybrid annual power load forecasting model based on generalized regression neural network with fruit fly optimization algorithm. *Knowl.-Based Syst.* **2013**, *37*, 378–387. [CrossRef]
86. Ibrić, S.; Djuriš, J.; Parojčić, J.; Djurić, Z. Artificial Neural Networks in Evaluation and Optimization of Modified Release Solid Dosage Forms. *Pharmaceutics* **2012**, *4*, 531–550. [CrossRef]
87. Sözen, A.; Arcaklioğlu, E.; Özalp, M.; Kanit, E.G. Use of artificial neural networks for mapping of solar potential in Turkey. *Appl. Energy* **2004**, *77*, 273–286. [CrossRef]
88. Ding, M.; Wang, L.; Bi, R. An ANN-based Approach for Forecasting the Power Output of Photovoltaic System. *Procedia Environ. Sci.* **2011**, *11*, 1308–1315. [CrossRef]
89. Bizzarri, F.; Bongiorno, M.; Brambilla, A.; Gruosso, G.; Gajani, G.S. Model of photovoltaic power plants for performance analysis and production forecast. *IEEE Trans. Sustain. Energy* **2013**, *4*, 278–285. [CrossRef]
90. Smolensky, P.; Mozer, M.; Rumelhart, D. *Mathematical Perspectives on Neural Networks*, 1st ed.; Taylor and Francis: Philadelphia, PA, USA, 2013; ISBN 9780203772966.
91. Srisaeng, P.; Baxter, G.; Wild, G. An adaptive neuro-fuzzy inference system for forecasting Australia's domestic low cost carrier passenger demand. *Vilnius Gedim. Tech. Univ.* **2015**, *19*, 150–163. [CrossRef]
92. Yun, Z.; Quan, Z.; Caixin, S.; Shaolan, L.; Yuming, L.; Yang, S. RBF neural network and ANFIS-based short-term load forecasting approach in real-time price environment. *IEEE Trans. Power Syst.* **2008**, *23*, 853–858.
93. Awadallah, M.; Soliman, H.; Ehab, M.; Bayoumi, H.; Soliman, H. Adaptive deadbeat controllers for brushless dc drives using PSO and ANFIS techniques. *J. Electr. Eng.* **2009**, *60*, 3–11.
94. Raza, M.Q.; Khosravi, A. A review on artificial intelligence-based load demand forecasting techniques for smart grid and buildings. *Renew. Sustain. Energy Rev.* **2015**, *50*, 1352–1372. [CrossRef]
95. De Giorgi, M.; Malvoni, M.; Congedo, P. Comparison of strategies for multi-step ahead photovoltaic power forecasting models based on hybrid group method of data handling networks and least square support vector machine. *Energy* **2016**, *107*, 360–373. [CrossRef]
96. Schölkopf, B.; Smola, A.; Müller, K. Kernel principal component analysis. In *Artificial Neural Networks*; Gerstner, W., Germond, A., Hasler, M., Nicoud, J., Eds.; Springer: Berlin/Heidelberg, Germany, 1997; Volume 1327, pp. 583–588. [CrossRef]
97. Vapnik, V. *The Nature of Statistical Learning Theory*, 2nd ed.; Springer: New York, NY, USA, 1999.
98. Hu, J.; Gao, P.; Yao, Y.; Xie, X. Traffic flow forecasting with particle swarm optimization and support vector regression. In Proceedings of the 17th International IEEE Conference on Intelligent Transportation Systems (ITSC), Qindao, China, 8–11 October 2014. [CrossRef]
99. Zhang, F.; Deb, C.; Lee, S.; Yang, J.; Shah, K. Time series forecasting for building energy consumption using weighted Support Vector Regression with differential evolution optimization technique. *Energy Build.* **2016**, *126*, 94–103. [CrossRef]
100. Hong, W. Electric load forecasting by support vector model. *Appl. Math. Model* **2009**, *33*, 2444–2454. [CrossRef]
101. Müller, K.; Smoła, A.; Rätsch, G.; Schölkopf, B.; Kohlmorgen, J.; Vapnik, V. Predicting time series with support vector machines. In *Artificial Neural Networks*; Gerstner, W., Germond, A., Hasler, M., Nicoud, J., Eds.; Springer: Berlin, Germany, 1997; Volume 1327, pp. 999–1004. [CrossRef]
102. Tang, Y.; Zhou, J. The performance of PSO-SVM in inflation forecasting. In Proceedings of the 12th International Conference on Service Systems and Service Management (ICSSSM), Guangzhou, China, 22–24 June 2015. [CrossRef]
103. Mao, M.; Gong, W.; Chang, L. Short-term photovoltaic output forecasting model for economic dispatch of power system incorporating large-scale photovoltaic plant. In Proceedings of the IEEE Energy Conversion Congress and Exposition, Denver, CO, USA, 15–19 September 2013. [CrossRef]
104. Lin, K.; Pai, P. Solar power output forecasting using evolutionary seasonal decomposition least-square support vector regression. *J. Clean. Prod.* **2016**, *134*, 456–462. [CrossRef]
105. Cherkassky, V.; Ma, Y. Practical selection of SVM parameters and noise estimation for SVM regression. *Neural Netw.* **2004**, *17*, 113–126. [CrossRef]
106. Yona, A.; Senjyu, T.; Funabashi, T.; Kim, C. Determination method of insolation prediction with fuzzy and applying neural network for long-term ahead PV power output correction. *IEEE Trans. Sustain. Energy* **2013**, *4*, 527–533. [CrossRef]

107. Chen, S.; Chang, Y.; Chen, Z.; Chen, C. Multiple fuzzy rules interpolation with weighted antecedent variables in sparse fuzzy rule-based systems. *Int. J. Pattern Recognit. Artif. Intell.* **2013**, *27*, 1359002. [CrossRef]
108. Colak, T.; Qahwaji, R. Automatic sunspot classification for real-time forecasting of solar activities. In Proceedings of the 2007 3rd International Conference on Recent Advances in Space Technologies RAST, Istanbul, Turkey, 14–16 June 2007. [CrossRef]
109. Liu, J.; Fang, W.; Zhang, X.; Yang, C. Photovoltaic Power Forecasting with a Hybrid Deep Learning Approach. *IEEE Access* **2020**, *8*, 175871–175880. [CrossRef]
110. Ali, M.; Mahmoud, K.; Lehtonen, M.; Access, M.D.-I. An efficient fuzzy-logic based variable-step incremental conductance MPPT method for grid-connected PV systems. *IEEE Access* **2021**, *9*, 26420–26430. [CrossRef]
111. Ali, M.; Mahmoud, K.; Lehtonen, M.; Sensors, M.D. Promising MPPT methods combining metaheuristic, fuzzy-logic and ANN techniques for grid-connected photovoltaic. *Sensors* **2021**, *21*, 1244. [CrossRef] [PubMed]
112. Bayoumi, A.; El-Sehiemy, R.; Sciences, K.M.-A. Assessment of an improved three-diode against modified two-diode patterns of MCS solar cells associated with soft parameter estimation paradigms. *Appl. Sci.* **2021**, *13*, 1055. [CrossRef]
113. Abbas, A.S.; El-Sehiemy, R.A.; Abou El-Ela, A.; Ali, E.S.; Mahmoud, K.; Lehtonen, M.; Darwish, M.M.F. Optimal Harmonic Mitigation in Distribution Systems with Inverter Based Distributed Generation. *Appl. Sci.* **2021**, *11*, 774. [CrossRef]
114. Qais, M.H.; Hasanien, H.M.; Alghuwainem, S. Transient search optimization for electrical parameters estimation of photovoltaic module based on datasheet values. *Energy Convers. Manag.* **2020**, *214*, 112904. [CrossRef]
115. Said, M.; Shaheen Abdullah, M.; Ginidi, A.R.; El-Sehiemy, R.A.; Mahmoud, K.; Lehtonen, M.; Darwish, M.M.F. Estimating Parameters of Photovoltaic Models Using Accurate Turbulent Flow of Water Optimizer. *Processes* **2021**, *9*, 627. [CrossRef]
116. Sudhakar Babu, T.; Prasanth Ram, J.; Sangeetha, K.; Laudani, A.; Rajasekar, N. Parameter extraction of two diode solar PV model using Fireworks algorithm. *Sol. Energy* **2016**, *140*, 265–276. [CrossRef]
117. Khanna, V.; Das, B.K.; Bisht, D.; Vandana; Singh, P.K. A three diode model for industrial solar cells and estimation of solar cell parameters using PSO algorithm. *Renew. Energy* **2015**, *78*, 105–113. [CrossRef]
118. AlRashidi, M.R.; AlHajri, M.F.; El-Naggar, K.M.; Al-Othman, A.K. A new estimation approach for determining the I–V characteristics of solar cells. *Sol. Energy* **2011**, *85*, 1543–1550. [CrossRef]
119. Lin, P.; Cheng, S.; Yeh, W.; Chen, Z.; Wu, L. Parameters extraction of solar cell models using a modified simplified swarm optimization algorithm. *Sol. Energy* **2017**, *144*, 594–603. [CrossRef]
120. Elsisi, M.; Mahmoud, K.; Lehtonen, M.; Access, M.D.-I. An improved neural network algorithm to efficiently track various trajectories of robot manipulator arms. *IEEE Access* **2021**, *9*, 11911–11920. [CrossRef]
121. Elsisi, M.; Mahmoud, K.; Lehtonen, M.; Sensors, M.D. Reliable industry 4.0 based on machine learning and IOT for analyzing, monitoring, and securing smart meters. *Sensors* **2021**, *21*, 487. [CrossRef] [PubMed]
122. Mansour, D.A.; Abdel-Gawad, N.M.; El Dein, A.Z.; Ahmed, H.M.; Darwish, M.M.F.; Lehtonen, M. Recent advances in polymer nanocomposites based on polyethylene and polyvinylchloride for power cables. *Materials* **2020**, *14*, 66. [CrossRef]
123. Abouelatta, M.; Ward, S.; Sayed, A.; Mahmoud, K. Fast corona discharge assessment using FDM integrated with full multigrid method in HVDC transmission lines considering wind impact. *IEEE Access* **2020**, *8*, 225872–225883. [CrossRef]
124. Ghoneim, S.; Mahmoud, K.; Lehtonen, M. Enhancing diagnostic accuracy of transformer faults using teaching-learning-based optimization. *IEEE Access* **2021**, *9*, 30817–30832. [CrossRef]
125. Abaza, A.; El-Sehiemy, R.A.; Mahmoud, K.; Lehtonen, M.; Darwish, M.M.F. Optimal estimation of proton exchange membrane fuel cells parameter based on coyote optimization algorithm. *Appl. Sci.* **2021**, *11*, 2052. [CrossRef]
126. Lun, S.X.; Wang, S.; Yang, G.H.; Guo, T.T. A new explicit double-diode modeling method based on Lambert W-function for photovoltaic arrays. *Sol. Energy* **2015**, *116*, 69–82. [CrossRef]
127. Et-torabi, K.; Nassar-eddine, I.; Obbadi, A.; Errami, Y.; Rmaily, R.; Sahnoun, S.; El Fajri, A.; Agunaou, M. Parameters estimation of the single and double diode photovoltaic models using a Gauss–Seidel algorithm and analytical method: A comparative study. *Energy Convers. Manag.* **2017**, *148*, 1041–1054. [CrossRef]
128. Kanimozhi, G.; Kumar, H. Modeling of solar cell under different conditions by Ant Lion Optimizer with LambertW function. *Appl. Soft Comput.* **2018**, *71*, 141–151.
129. Toledo, F.; Blanes, J.; Galiano, V. Two-step linear least-squares method for photovoltaic single-diode model parameters extraction. *IEEE Trans. Ind. Electron.* **2018**, *65*, 6301–6308. [CrossRef]
130. Ayang, A.; Wamkeue, R.; Ouhrouche, M.; Djongyang, N.; Essiane Salomé, N.; Pombe, J.K.; Ekemb, G. Maximum likelihood parameters estimation of single-diode model of photovoltaic generator. *Renew. Energy* **2019**, *130*, 111–121. [CrossRef]
131. Guo, L.; Meng, Z.; Sun, Y.; Wang, L. Parameter identification and sensitivity analysis of solar cell models with cat swarm optimization algorithm. *Energy Convers. Manag.* **2016**, *108*, 520–528. [CrossRef]
132. Ebrahimi, S.M.; Salahshour, E.; Malekzadeh, M.; Gordillo, F. Parameters identification of PV solar cells and modules using flexible particle swarm optimization algorithm. *Energy* **2019**, *179*, 358–372. [CrossRef]
133. Abbassi, R.; Abbassi, A.; Heidari, A.A.; Mirjalili, S. An efficient salp swarm-inspired algorithm for parameters identification of photovoltaic cell models. *Energy Convers. Manag.* **2019**, *179*, 362–372. [CrossRef]
134. Xiong, G.; Zhang, J.; Yuan, X.; Shi, D.; He, Y.; Yao, G. Parameter extraction of solar photovoltaic models by means of a hybrid differential evolution with whale optimization algorithm. *Sol. Energy* **2018**, *176*, 742–761. [CrossRef]
135. Gao, X.; Cui, Y.; Hu, J.; Xu, G.; Wang, Z.; Qu, J.; Wang, H. Parameter extraction of solar cell models using improved shuffled complex evolution algorithm. *Energy Convers. Manag.* **2018**, *157*, 460–479. [CrossRef]

136. Liang, J.; Qiao, K.; Yu, K.; Ge, S.; Qu, B.; Xu, R.; Li, K. Parameters estimation of solar photovoltaic models via a self-adaptive ensemble-based differential evolution. *Sol. Energy* **2020**, *207*, 336–346. [CrossRef]
137. Abbassi, A.; Abbassi, R.; Heidari, A.A.; Oliva, D.; Chen, H.; Habib, A.; Jemli, M.; Wang, M. Parameters identification of photovoltaic cell models using enhanced exploratory salp chains-based approach. *Energy* **2020**, *198*, 117333. [CrossRef]
138. Yu, K.; Liang, J.J.; Qu, B.Y.; Cheng, Z.; Wang, H. Multiple learning backtracking search algorithm for estimating parameters of photovoltaic models. *Appl. Energy* **2018**, *226*, 408–422. [CrossRef]
139. Zhang, H.; Heidari, A.A.; Wang, M.; Zhang, L.; Chen, H.; Li, C. Orthogonal Nelder-Mead moth flame method for parameters identification of photovoltaic modules. *Energy Convers. Manag.* **2020**, *211*, 112764. [CrossRef]
140. Zaky, A.A.; El Sehiemy, R.A.; Rashwan, Y.I.; Elhossieni, M.A.; Gkini, K.; Kladas, A.; Falaras, P. Optimal Performance Emulation of PSCs using the Elephant Herd Algorithm Associated with Experimental Validation. *ECS J. Solid State Sci. Technol.* **2019**, *8*, Q249–Q255. [CrossRef]
141. Jian, X.; Weng, Z. A logistic chaotic JAYA algorithm for parameters identification of photovoltaic cell and module models. *Optik* **2020**, *203*, 164041. [CrossRef]
142. Chen, H. An opposition-based sine cosine approach with local search for parameter estimation of photovoltaic models. *Energy Convers. Manag.* **2019**, *195*, 927–942. [CrossRef]
143. Oliva, D.; Ewees, A.A.; Abd El Aziz, M.; Hassanien, A.E.; Cisneros, M.P. A chaotic improved artificial bee colony for parameter estimation of photovoltaic cells. *Energies* **2017**, *10*, 865. [CrossRef]
144. Niu, Q.; Zhang, H.; Li, K. An improved TLBO with elite strategy for parameters identification of PEM fuel cell and solar cell models. *Int. J. Hydrogen Energy* **2014**, *39*, 3837–3854. [CrossRef]
145. Allam, D.; Yousri, D.A.; Eteiba, M.B. Parameters extraction of the three diode model for the multi-crystalline solar cell/module using Moth-Flame Optimization Algorithm. *Energy Convers. Manag.* **2016**, *123*, 535–548. [CrossRef]
146. Ghasemi, M. A novel and effective optimization algorithm for global optimization and its engineering applications: Turbulent Flow of Water-based Optimization (TFWO). *Eng. Appl. Artif. Intell.* **2020**, *92*, 10366. [CrossRef]
147. Abdollahzadeh, B.; Soleimanian Gharehchopogh, F.; Mirjalili, S. Artificial gorilla troops optimizer: A new nature-inspired metaheuristic algorithm for global optimization problems. *Int. J. Intell. Syst.* **2021**, *36*, 5887–5958. [CrossRef]
148. Ginidi, A.R.; Shaheen, A.M.; El-Sehiemy, R.A.; Elattar, E. Supply demand optimization algorithm for parameter extraction of various solar cell models. *Energy Rep.* **2021**, *7*, 5772–5794. [CrossRef]
149. Askari, Q.; Saeed, M.; Younas, I. Heap-based optimizer inspired by corporate rank hierarchy for global optimization. *Expert Syst. Appl.* **2020**, *161*, 113702. [CrossRef]
150. Chin, V.J.; Salam, Z. Coyote optimization algorithm for the parameter extraction of photovoltaic cells. *Sol. Energy* **2019**, *194*, 656–670. [CrossRef]
151. Ginidi, A.; Shaheen, A.; El-Sehiemy, R.; El-Fergany, A. Gorilla troops optimizer for electrically based single and double-diode models of solar photovoltaic systems. *Sustainability* **2021**, *13*, 9459. [CrossRef]
152. Liu, J.; Fang, W.; Zhang, X.; Yang, C. An Improved Photovoltaic Power Forecasting Model with the Assistance of Aerosol Index Data. *IEEE Trans. Sustain. Energy* **2015**, *6*, 434–442. [CrossRef]
153. Yang, C.; Thatte, A.; Xie, L. Multitime-scale data-driven spatio-temporal forecast of photovoltaic generation. *IEEE Trans. Sustain. Energy* **2015**, *6*, 104–112. [CrossRef]
154. Leva, S.; Dolara, A.; Grimaccia, F.; Mussetta, M.; Ogliari, E. Analysis and validation of 24 hours ahead neural network forecasting of photovoltaic output power. *Math. Comput. Simul.* **2017**, *131*, 88–100. [CrossRef]
155. Mashud, M.; Koprinska, I.; Georgios Agelidis, V.; Rana, M.; Agelidis, V. Forecasting solar power generated by grid connected PV systems using ensembles of neural networks. In Proceedings of the International Joint Conference on Neural Networks (IJCNN), Killarney, Ireland, 12–17 July 2015. [CrossRef]
156. Almeida, M.; Perpinan, O.; Narvarte, L. PV power forecast using a nonparametric PV model. *Sol. Energy* **2015**, *115*, 354–368. [CrossRef]
157. Reikard, G. Predicting solar radiation at high resolutions: A comparison of time series forecasts. *Sol. Energy* **2009**, *83*, 342–349. [CrossRef]
158. Ghofrani, M.; Ghayekhloo, M.; Azimi, R. A novel soft computing framework for solar radiation forecasting. *Appl. Soft Comput.* **2016**, *48*, 207–216. [CrossRef]
159. Gupta, A.; Chauhan, Y.; Pachauri, R. A comparative investigation of maximum power point tracking methods for solar PV system. *Sol. Energy* **2016**, *136*, 236–253. [CrossRef]
160. Law, E.; Prasad, A.; Kay, M.; Taylor, R. Direct normal irradiance forecasting and its application to concentrated solar thermal output forecasting—A review. *Sol. Energy* **2014**, *108*, 287–307. [CrossRef]
161. Chen, P.; Yuan, L.; He, Y.; Luo, S. An improved SVM classifier based on double chains quantum genetic algorithm and its application in analogue circuit diagnosis. *Neurocomputing* **2016**, *211*, 202–211. [CrossRef]
162. Li, Y.; He, Y.; Su, Y.; Shu, L. Forecasting the daily power output of a grid-connected photovoltaic system based on multivariate adaptive regression splines. *Appl. Energy* **2016**, *180*, 392–401. [CrossRef]
163. Lauret, P.; Voyant, C.; Soubdhan, T.; David, M.; Poggi, P. A benchmarking of machine learning techniques for solar radiation forecasting in an insular context. *Sol. Energy* **2015**, *112*, 446–457. [CrossRef]

164. Mojumder, J.; Ong, H.; Chong, W.; Shamshirband, S.; Al-Mamoon, A. Application of support vector machine for prediction of electrical and thermal performance in PV/T system. *Energy Build.* **2016**, *111*, 267–277. [CrossRef]
165. Daye, T. Managing intermittency: Standards and recommended practices in solar power forecasting. *ERCOT Emerg. Technol.* 2011. Available online: https://energy.mit.edu/wp-content/uploads/2012/03/MITEI-RP-2011-001.pdf (accessed on 13 October 2022).
166. Ratshilengo, M.; Sigauke, C.; Bere, A. Short-Term Solar Power Forecasting Using Genetic Algorithms: An Application Using South African Data. *Appl. Sci.* **2021**, *11*, 4214. [CrossRef]
167. Zhang, J.; Verschae, R.; Nobuhara, S.; Lalonde, J. Deep photovoltaic nowcasting. *Sol. Energy* **2018**, *176*, 267–276. [CrossRef]
168. El Hendouzi, A.; Bourouhou, A.; Ansari, O. The Importance of Distance between Photovoltaic Power Stations for Clear Accuracy of Short-Term Photovoltaic Power Forecasting. *J. Electr. Comput. Eng.* **2020**, *2020*, 9586707. [CrossRef]
169. Luo, X.; Zhang, D.; Zhu, X. Deep learning based forecasting of photovoltaic power generation by incorporating domain knowledge. *Energy* **2021**, *225*, 120240. [CrossRef]
170. Dawan, P.; Sriprapha, K.; Kittisontirak, S.; Boonraksa, T.; Junhuathon, N.; Titiroongruang, W.; Niemcharoen, S. Comparison of Power Output Forecasting on the Photovoltaic System Using Adaptive Neuro-Fuzzy Inference Systems and Particle Swarm Optimization-Artificial Neural Network Model. *Energies* **2020**, *13*, 351. [CrossRef]
171. Bessa, R.J.; Trindade, A.; Silva, C.S.P.; Miranda, V. Probabilistic solar power forecasting in smart grids using distributed information. *Int. J. Electr. Power Energy Syst.* **2015**, *72*, 16–23. [CrossRef]
172. Chupong, C.; Plangklang, B. Forecasting power output of PV grid connected system in Thailand without using solar radiation measurement. *Energy Procedia* **2011**, *9*, 230–237. [CrossRef]
173. Semero, Y.; Zhang, J.; Zheng, D. PV power forecasting using an integrated GA-PSO-ANFIS approach and Gaussian process regression based feature selection strategy. *CSEE J. Power Energy Syst.* **2018**, *4*, 210–218. [CrossRef]
174. Zhu, H.; Li, X.; Sun, Q.; Nie, L.; Yao, J.; Zhao, G. A Power Prediction Method for Photovoltaic Power Plant Based on Wavelet Decomposition and Artificial Neural Networks. *Energies* **2016**, *9*, 11. [CrossRef]
175. Xu, Q.; He, D.; Zhang, N.; Kang, C.; Xia, Q.; Bai, J.; Huang, J. A short-term wind power forecasting approach with adjustment of numerical weather prediction input by data mining. *IEEE Trans. Sustain. Energy* **2015**, *6*, 1283–1291. [CrossRef]
176. Zamo, M.; Mestre, O.; Arbogast, P.; Pannekoucke, O. A benchmark of statistical regression methods for short-term forecasting of photovoltaic electricity production. Part II: Probabilistic forecast of daily production. *Sol. Energy* **2014**, *105*, 804–816. [CrossRef]
177. Chen, C.; Duan, S.; Cai, T.; Liu, B. Online 24-h solar power forecasting based on weather type classification using artificial neural network. *Sol. Energy* **2011**, *85*, 2856–2870. [CrossRef]
178. Haque, A.; Nehrir, M.; Mandal, P. Solar PV power generation forecast using a hybrid intelligent approach. In Proceedings of the IEEE Power Energy Society General Meeting, Vancouver, BC, Canada, 21–25 July 2013. [CrossRef]
179. Tao, Y.; Chen, Y. Distributed PV power forecasting using genetic algorithm based neural network approach. In Proceedings of the International Conference on Advanced Mechatronic Systems ICAMechS, Kumamoto, Japan, 10–12 August 2014. [CrossRef]
180. Ramsami, P.; Oree, V. A hybrid method for forecasting the energy output of photovoltaic systems. *Energy Convers. Manag.* **2015**, *95*, 406–413. [CrossRef]
181. Nagi, J.; Yap, K.; Tiong, S.; Ahmed, S. Electrical power load forecasting using hybrid self-organizing maps and support vector machines. In Proceedings of the International Power Engineering and Optimization Conference, Selangor, Malaysia, 4–5 June 2008.
182. Xu, R.; Chen, H.; Sun, X. Short-term photovoltaic power forecasting with weighted support vector machine. In Proceedings of the IEEE International Conference on Automation and Logistics ICAL, Zhengzhou, China, 15–17 August 2012.
183. Qiongbing, Z.; Lixin, D. A new crossover mechanism for genetic algorithms with variable-length chromosomes for path optimization problems. *Expert Syst. Appl.* **2016**, *60*, 183–189. [CrossRef]
184. Bashir, Z.A.; El-Hawary, M.E. Applying wavelets to short-term load forecasting using PSO-based neural networks. *IEEE Trans. Power Syst.* **2009**, *24*, 20–27. [CrossRef]
185. Hong, W. Electric load forecasting by seasonal recurrent SVR (support vector regression) with chaotic artificial bee colony algorithm. *Energy* **2011**, *36*, 5568–5578. [CrossRef]
186. Bao, Y.; Liu, Z. A Fast Grid Search Method in Support Vector Regression Forecasting Time Series. In *Intelligent Data Engineering and Automated Learning*; Corchado, E., Yin, H., Botti, V., Fyfe, C., Eds.; Springer: Berlin, Germany, 2006; Volume 4224, pp. 504–511.
187. Hong, W. Application of chaotic ant swarm optimization in electric load forecasting. *Energy Policy* **2010**, *38*, 5830–5839. [CrossRef]
188. Niu, D.; Wang, Y.; Wu, D. Power load forecasting using support vector machine and ant colony optimization. *Expert Syst. Appl.* **2010**, *37*, 2531–2539. [CrossRef]
189. Ye, H.; Yang, B.; Han, Y.; Chen, N. State-Of-The-Art Solar Energy Forecasting Approaches: Critical Potentials and Challenges. *Front. Energy Res.* **2022**, *10*, 268.